

AD-A139 015

NEUTRON LEAKAGE FROM 'COMET' - A DUPLICATE LITTLE-BOY
DEVICE(U) DEFENCE RESEARCH ESTABLISHMENT OTTAWA
(ONTARIO) H A ROBITAILLE ET AL. DEC 83 DREQ-878

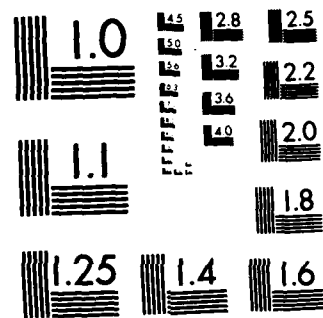
1//

UNCLASSIFIED

F/G 6/18

NL

END
DATE
FILED
4 84
DRC



MICROCOPY RESOLUTION TEST CHART
NATIONAL BUREAU OF STANDARDS-1963-A

AD A 139015



National
Defence

Défense
nationale



(3)

NEUTRON LEAKAGE FROM "COMET"- A DUPLICATE LITTLE-BOY DEVICE

by

H.A. Robitaille and B.E. Hoffarth



DTIC FILE COPY

Canada

DEFENCE RESEARCH ESTABLISHMENT OTTAWA
REPORT 878

This document has been approved
for public release and sale; its
distribution is unlimited.

December 1983
Ottawa

84 03 13 303



National
Defence Défense
nationale

NEUTRON LEAKAGE FROM "COMET"- A DUPLICATE LITTLE-BOY DEVICE

by

H.A. Robitaille and B.E. Hoffarth
Nuclear Effects Section
Protective Sciences Division

Accession For	
NTIS	GRA&I
DTIC	TAB
Unannounced	
Justification	
By _____	
Distribution/ _____	
Availability Codes	
Dist	Avail and/or Special
A-1	



DEFENCE RESEARCH ESTABLISHMENT OTTAWA
REPORT 878

PCN
11A

December 1983
Ottawa

ABSTRACT

Fast neutron spectra between 600 keV and 10 MeV, directed outwards from the surface of the "COMET" assembly, were measured using an NE-213 fast-neutron spectrometer at the Los Alamos National Laboratory. The COMET experiment, consisting of a duplicate Little-Boy device suitably modified for operation in the delayed-critical regime, was to provide improved energy and angular distributions of leakage spectra in support of efforts to re-evaluate ground doses from the Hiroshima bombing.

Measurements were obtained at seven polar angles (from 0 to 135 degrees) and at two radii from the centre of the active volume (75 and 200 centimeters). These measurements were compared to two calculations available at the time of writing; one an earlier (1976) one-dimensional estimation and another more recent (1982) two-dimensional calculation, both based on Monte-Carlo techniques. Differences in high-energy neutron leakage are apparent and probably due to dynamical considerations, as the theoretical calculations simulated the disassembling weapon itself, rather than the static experiments described herein.

RÉSUMÉ

Les spectres de neutrons rapides de 600 keV à 10 MeV émergent de la surface du "COMET" ont été établis au spectromètre de recul protonique NE-213 au Laboratoire National de Los Alamos. L'expérience COMET, constituée d'une reproduction de Little-Boy modifiée pour fonctionner en régime critique pour les neutrons retardés, devait fournir des distributions énergétiques et angulaires améliorées des spectres de fuite pour aider à réévaluer les doses au sol lors du bombardement d'Hiroshima.

Des mesures ont été prises sous sept angles polaires (compris entre 0 et 135 degrés) et à deux distances du centre du volume actif (rayons de 75 et de 200 centimètres). Ces mesures ont été comparées à deux calculs disponibles au moment d'écrire ces lignes: une estimation unidimensionnelle de 1976 et une bidimensionnelle plus récente de 1982, toutes deux basées sur des techniques de Monte-Carlo. Il existe des différences apparentes dans la fuite des neutrons de haute énergie, différences qui sont probablement dues à des facteurs dynamiques, puisque les calculs théoriques simulaient l'arme elle-même plutôt que les expériences statiques décrites ici.

TABLE OF CONTENTS

	<u>Page</u>
INTRODUCTION	1
EXPERIMENT	2
RESULTS	4
Angular Distributions of Fluence and Kerma	5
Neutron Spectra Integrated Over Angle	9
Boron-triflouride Detector Counting Data	10
COMPARISON TO THEORETICAL CALCULATIONS	12
CONCLUSIONS	15
REFERENCES	16
APPENDIX A. Plotted Neutron Spectra	19
APPENDIX B. Listed Neutron Spectra	27
APPENDIX C. Boron-triflouride Detector Efficiency	35

LIST OF ILLUSTRATIONS

	<u>Page</u>
Figure 1 : Detector locations surrounding the COMET assembly at which neutron spectra were obtained	3
Figure 2 : Polar distribution of neutron fluence above 600 keV	7
Figure 3 : Polar distribution of neutron kerma above 600 keV	8
Figure 4 : Neutron spectra integrated over angle	9
Figure 5 : Comparison of 75-cm leakage spectrum to calculations	13
Figure 6 : Comparison of 200-cm leakage spectrum to calculations	14
Figure A-1 : Neutron spectrum at 0 degrees and 75 cm	19
Figure A-2 : Neutron spectrum at 22.5 degrees and 75 cm	20
Figure A-3 : Neutron spectrum at 45 degrees and 75 cm	20
Figure A-4 : Neutron spectrum at 67.5 degrees and 75 cm	21
Figure A-5 : Neutron spectrum at 90 degrees and 75 cm	21
Figure A-6 : Neutron spectrum at 112.5 degrees and 75 cm	22
Figure A-7 : Neutron spectrum at 135 degrees and 75 cm	22
Figure A-8 : Neutron spectrum at 0 degrees and 200 cm	23
Figure A-9 : Neutron spectrum at 45 degrees and 200 cm	23
Figure A-10 : Neutron spectrum at 67.5 degrees and 200 cm	24
Figure A-11 : Neutron spectrum at 90 degrees and 200 cm	24
Figure A-12 : Neutron spectrum at 112.5 degrees and 200 cm	25
Figure A-13 : Neutron spectrum at 135 degrees and 200 cm	25
Figure A-14 : Neutron leakage spectrum at 75 cm	26
Figure A-15 : Neutron leakage spectrum at 200 cm	26
Figure C-1 : Energy-dependent detection efficiency for the Cd-covered BF_3 detector	36

LIST OF TABLES

	<u>Page</u>
Table 1 : Weighting factors for angular integrations	4
Table 2 : Integral quantities determined above 600 keV	6
Table 3 : Cadmium-covered boron-triflouride detector counting-rates	11
Table B-1 : COMET Neutron spectrum at 0 degrees and 75 cm	27
Table B-2 : COMET Neutron spectrum at 22.5 degrees and 75 cm	28
Table B-3 : COMET Neutron spectrum at 45 degrees and 75 cm	28
Table B-4 : COMET Neutron spectrum at 67.5 degrees and 75 cm	29
Table B-5 : COMET Neutron spectrum at 90 degrees and 75 cm	29
Table B-6 : COMET Neutron spectrum at 112.5 degrees and 75 cm	30
Table B-7 : COMET Neutron spectrum at 135 degrees and 75 cm	30
Table B-8 : COMET Neutron spectrum at 0 degrees and 200 cm	31
Table B-9 : COMET Neutron spectrum at 45 degrees and 200 cm	31
Table B-10 : COMET Neutron spectrum at 67.5 degrees and 200 cm	32
Table B-11 : COMET Neutron spectrum at 90 degrees and 200 cm	32
Table B-12 : COMET Neutron spectrum at 112.5 degrees and 200 cm	33
Table B-13 : COMET Neutron spectrum at 135 degrees and 200 cm	33
Table B-14 : Angle-integrated neutron spectrum at 75 cm	34
Table B-15 : Angle-integrated neutron spectrum at 200 cm	34
Table C-1 : Energy-dependent detection efficiency for the cadmium-covered boron-triflouride detector	37

INTRODUCTION

Recent estimates [1-6] of the radiation doses received by the survivors of the Hiroshima and Nagasaki bombings represent a substantial improvement in accuracy and confidence over previous dosimetric studies [7]. To a large extent this is due to advances in the intervening years in theoretical radiation transport codes and refinements in the nuclear interaction data available for such calculations. A 1981 review [5] suggested that further improvements in accuracy would be possible if more detailed investigations of the following parameters were undertaken :

1. Organ-dose factors (relationships of incident tissue kerma to internal doses at biologically-significant sites).
2. House-shielding factors (attenuation of incident tissue kerma by surrounding structures).
3. Energy yield of Little-Boy (since the Hiroshima bombing represented the sole detonation of this weapon design its yield is less certain than that of the Nagasaki device).
4. Neutron leakage from Little-Boy (previous 1-D calculations were unable to account for the anisotropy of neutron production from the cylindrically-symmetric device).

In order to validate the theoretical models used to refine the estimated yield and neutron leakage from the Little-Boy device (points 3 & 4 above) additional experimental information was desired [8]. This was to be provided by a duplicate Little-Boy warhead modified to operate as a delayed-critical experiment at the Critical Assembly Facility of the Los Alamos National Laboratory. Measurements of spectra, fluence and dose obtained at various positions surrounding the casing could then be compared to the predictions of corresponding two-dimensional calculations of the experimental assembly. Thus validated in the case of the "cold" (zero-yield) weapon, the calculational model could then be applied to the associated problem of predicting the leakage energy spectra and anisotropy of neutron production during the detonation of the super-critical device at Hiroshima.

Although differences in spectra between the two cases were anticipated [8], the experiment nevertheless tests the applicability of the theoretical codes and nuclear data to deal with radiation transport within the identical material composition used in the construction of the Little-Boy weapon.

A number of experimental groups were invited to participate in these measurements, including those from the Oak Ridge National Laboratory (ORNL), Lawrence Livermore National Laboratory (LLNL),

Los Alamos National Laboratory (LANL) and the Defence Research Establishment Ottawa (DREO). This report describes the measurements performed by DREO during September and October of 1982, as part of this effort.

EXPERIMENT

Fast neutron spectra (above an energy of 600 keV) were measured using a 2" x 1.75" NE-213 organic scintillator at the thirteen locations surrounding the casing shown in Figure 1. Pulse-height data were unfolded using an on-line code [9] and response matrix [10] previously developed at DREO. Additional integral information was provided by a cadmium-covered boron-triflouride counter of one-inch diameter and eight-inch sensitive length, enriched in the concentration of boron-10.

At a core-centre to detector separation of 200 centimeters estimation of the contribution of background neutrons (i.e. those interacting with the detectors after scattering off the walls and floor of the containment building) was accomplished by interposing a concrete block (36" x 36" x 18") between the source and detector. Such a thickness of concrete reduces the transmitted fast-neutron fluence by a factor of approximately one hundred [11], thus rendering the detectors sensitive primarily to room-scattered radiation. At 200 cm the NE-213 detector was influenced by an observed background contribution of 14 % of the total couting rate (>600 keV) at the 90 degree measurement location. The background contribution to the BF_3 detector was considerable higher, at about 65 %. Similar background corrections were obtained at all the other 200-cm locations with the sole exception of the position at 0 degrees, safety considerations prohibiting location of the block directly above the casing. At this particular location the background contribution was expected to be much lower as the casing itself shielded the detector from the floor beneath, from which a large portion of the scattered neutrons was suspected to originate.

At the 75-cm radius shadow-bar substitution measurements were impossible due to the close proximity of the detectors to the assembly casing. However at this closer distance the average neutron count rate (as seen by the NE-213 detector) was observed to increase by a factor of 6.5 compared to that at 200 cm. Since the background counting rate alone is expected to be relatively invariant to such a change in distance (most scattered neutrons originating from the walls and floor) the average background contribution at 75 cm was thus estimated to be no more than 2 % of the observed foreground counting rate. No background correction to the NE-213 measurements at 75 centimeters was therefore required. Similarly the background contribution to the BF_3 measurements at 75 cm was estimated to be approximately 20 % of the observed counting rate. This was considered by several approximations to be discussed later.

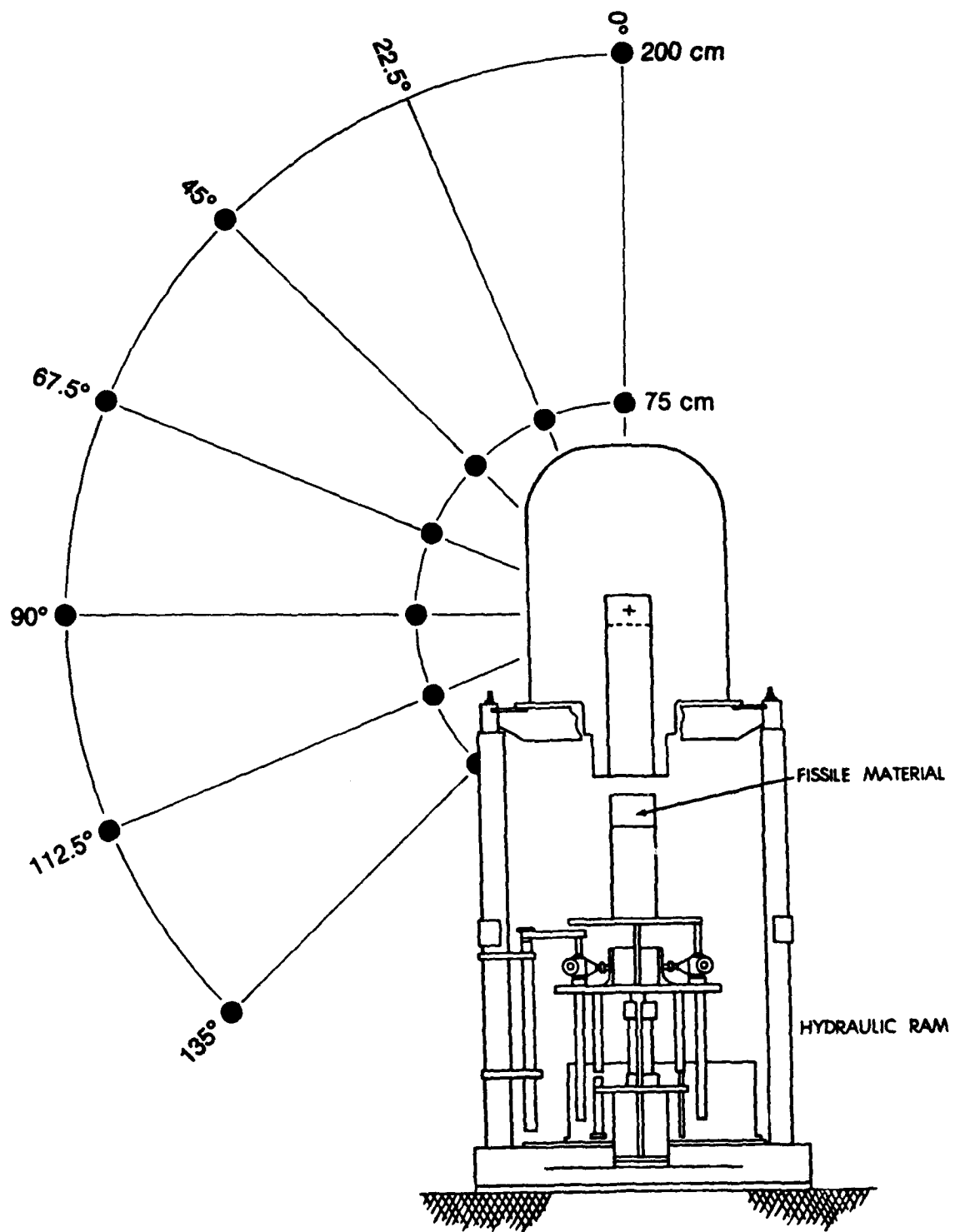


Figure 1 : Detector locations (●) surrounding the COMET assembly at which neutron spectra were obtained.

For each measurement the assembly power level was chosen such that maximum instrumental dead-time fractions were maintained below 5 %, and suitable dead-time corrections were applied at the time of data analysis. The assembly was operated without a startup neutron source and all other sources of any significance were removed from the experimental chamber. Unfolded data were subsequently normalized to the measured total fission rates, as determined by LANL, to within an estimated accuracy of 10 % (using a calibration factor of 6.35E-8 counts per fission for LANL fission chamber # 3) [12].

RESULTS

In subsequent discussions of the measurement results, occasionally referenced are quantities described as having been "integrated over angle". These angular integrations are by necessity approximate, and result from the weighted summation of quantities measured at similar core-centre to detector separations, but in differing directions. The weighting factors are determined by assuming no azimuthal variation in measured quantities (since the device is cylindrically-symmetric), and further assuming that quantities measured in a specific direction are invariant to change in polar direction, within specified limits. The individual weighting factors are numerically equal to elements of area to be associated with each detector location, on the surface of an imaginary sphere surrounding the casing with radius equal to the source-to-detector distance. Thus, the results of such angular integrations indicate the total leakage outwards from the casing, as determined at particular radii. The angular limits and weighting factors attributable to each detector location are tabulated below :

Angle ----- (degrees)	Angular Range ----- (degrees)	Weight (cm ²)		Relative Weight -----
		75 cm -----	200 cm -----	
0.0	0.0 - 11.25	679	4828	0.010
22.5	11.25 - 33.75	5277	37525	0.075
45.0	33.75 - 56.25	9751	69340	0.138
67.5	56.25 - 78.75	12740	90598	0.180
90.0	78.75 - 101.25	13790	98063	0.195
112.5	101.25 - 123.75	12740	90598	0.180
135.0	123.75 - 180.00	15707	111697	0.222
		-----	-----	-----
		70684	502649	1.000

Table 1 : Weighting factors for angular integrations.

Where data in a specific direction are unavailable, individual weighting factors are split equally and combined with the weights characteristic of neighbouring directions, such as in the case of the 22.5 degree direction at 200 cm for which no measurements were performed. In this case one-half of the weight at 22.5 degrees was added to the weight at 0 degrees and the other half to the weight at 45 degrees. The greatest approximation in this scheme is apparent at the 135 degree direction, to which is associated the range from 123.75 to 180 degrees, the casing stand and tamper drive motors having precluded measurements directly below the assembly. Nevertheless, the scheme permits consistent comparison between data measured at 75 cm and data at 200 cm, both having been treated with the same approximation.

If all escaping radiation originated at a point source and travelled directly to the detector without further interaction, the results of the angular integrations would be invariant with respect to change in detector distance and thus integrations performed at 200 cm would exactly equal those at 75 cm. Since this is clearly not the case, some variation with separation is in fact expected. In particular, at 75 cm a point detector would view an azimuthal range of the casing surface amounting to 12 degrees, whereas at 200 cm the detector would see 160 degrees of the casing circumference. (Infinitely far away the detector would view exactly one-half, or 180 degrees of the casing circumference). It is therefore expected that measurements at 200 cm should exceed somewhat those at 75 cm, due to failure of the "1/r²" law in this geometry. The exact increase to be expected is not easily estimated since this depends on the particular angular distribution of escaping radiation at the assembly surface, even if this is azimuthally invariant.

Angular Distributions of Fluence and Kerma

Individual neutron spectra measured at each location are shown plotted in Appendix A and listed in Appendix B. Neutron fluences and kermas above 600 keV derived by integration of these spectra against the appropriate fluence-to-kerma conversion factors [13] are tabulated below :

Angle (degrees)	Neutron Fluence		Neutron Kerma	
	(n/cm ² .fission)		(rad/fission)	
	75 cm	200 cm	75 cm	200 cm
0.0	2.58-7	4.11-8	5.30-16	9.12-17
22.5	2.11-7	-	4.33-16	-
45.0	4.89-7	8.77-8	1.05-15	1.90-16
67.5	1.01-6	1.52-7	2.21-15	3.32-16
90.0	1.32-6	1.82-7	2.94-15	4.03-16
112.5	1.11-6	1.71-7	2.45-15	3.75-16
135.0	7.97-7	1.32-7	1.72-15	2.87-16
$4\pi r^2$ Integral	0.0638	0.0726	1.39-10	1.55-10
	(neutrons/fission)		(rad.cm ² /fission)	

Table 2 : Integral quantities determined above 600 keV.

The statistical uncertainty associated with each of these quantities is not more than one percent, however a possible systematic uncertainty of up to 12 percent must be attributed to a combination of detector calibration and specific core power level uncertainties.

These integral quantities are also shown plotted in Figures 2 (fluence) and 3 (kerma). Quantities measured at a radius of 200 cm are seen to increase by approximately a factor of 4.5 from the 0 degree (nose) to 90 degree (side) measurement locations. Anisotropy indicated by the 75-cm measurements is somewhat higher, about a factor of 5.5. In closer proximity (75 cm) the detector is relatively more sensitive to the scalar fluence at the surface of the casing, whereas at the greater radius (200 cm) the detector is primarily sensitive to the angular distribution of escaping radiation, integrated over the surface of the casing as seen by the detector. It is therefore not surprising that the indicated degree of anisotropy decreases somewhat as the detector is moved farther from the casing.

Near a polar angle of 22.5 degrees a slight local minimum is apparent (in the 75-cm measurements) in both fluence and kerma. This is also reasonable since near this angle the optical path length through the casing from the core centre is greatest as the detector rounds the "corner" of the casing (Figure 1).

The degree of anisotropy of 4.5 noted at 200 cm may be compared to that measured in an earlier experiment employing a californium-252 neutron source at the centre of a similar Little-Boy casing [14]. In that experiment the indicated degree of anisotropy between 0 degree and 90 degree measurements at 200 cm was lower and equalled approximately a factor of 3. Since the measurements were performed with integral fluence monitors sensitive to lower energies

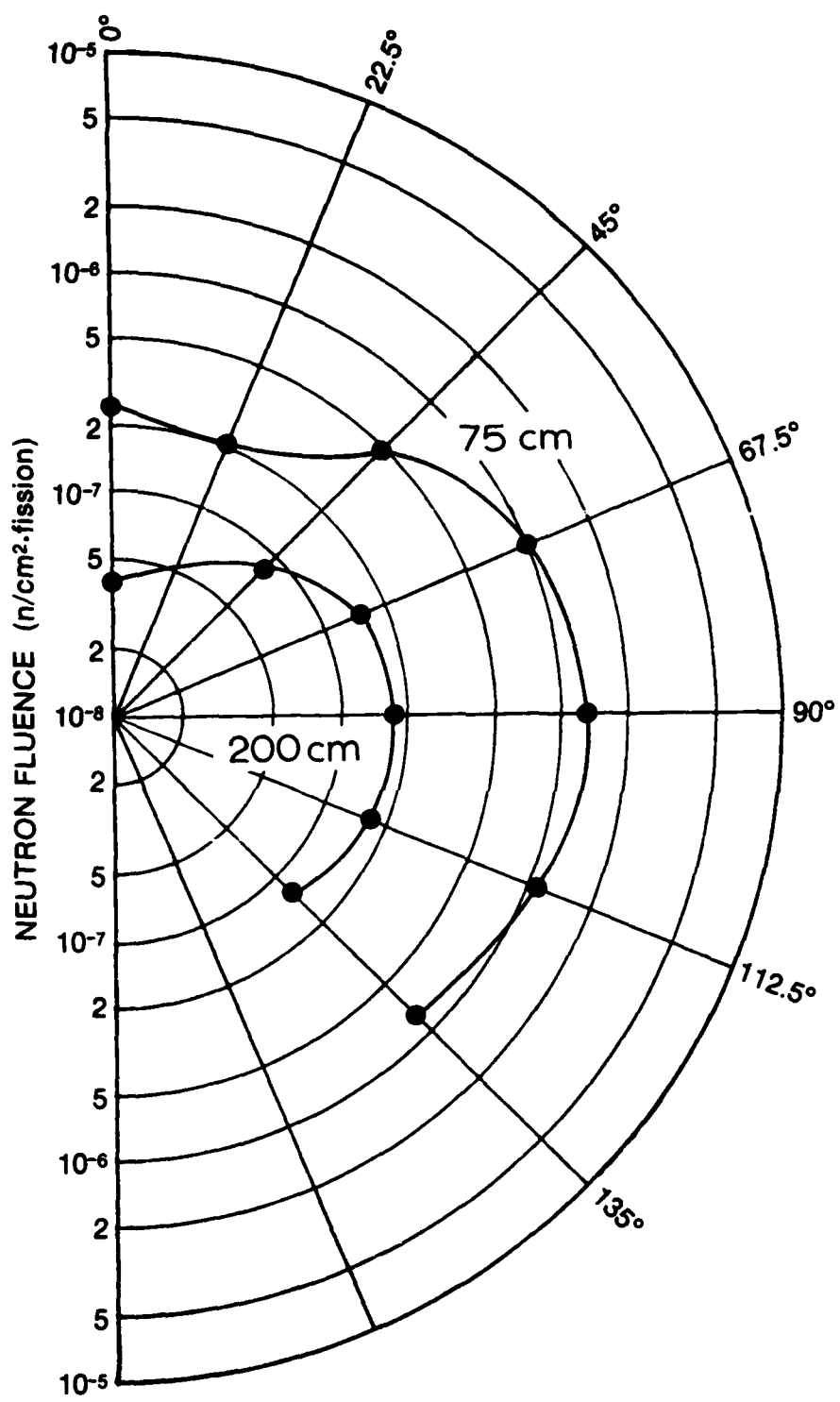


Figure 2 : Polar distribution of neutron fluence above 600 keV.

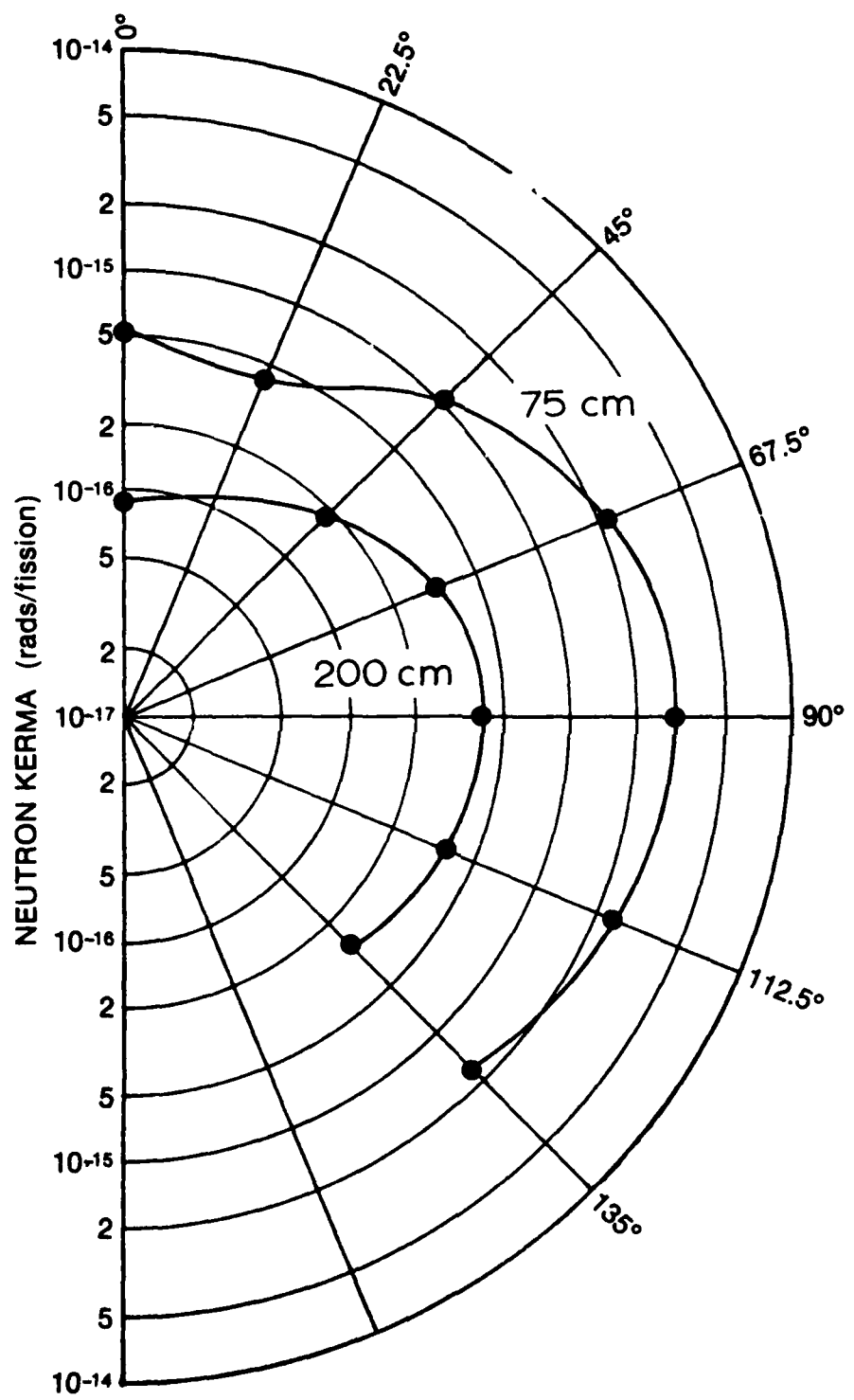


Figure 3 : Polar distribution of neutron kerma above 600 keV.

(1 keV), the additional contribution of primarily multiply-scattered neutrons would tend to decrease the apparent anisotropy.

As listed in Table 2, angularly-integrated quantities are seen to increase slightly from 75 to 200 cm. Both total fluence and kerma above 600 keV increase by 11 % as the detector is moved farther from the casing. As noted previously, this is consistent with the expected variation from "1/r²" behaviour.

Neutron Spectra Integrated Over Angle

Neutron spectra measured at 75 cm and 200 cm have also been integrated over direction according to the weighting factors of Table 1, and in a fashion similar to that described earlier. These are compared below (Figure 4), in which the spectrum obtained at 75 cm is shown as a solid line and the comparable spectrum at 200 cm as a broken line. The corresponding numerical data so derived are also listed in Appendix B.

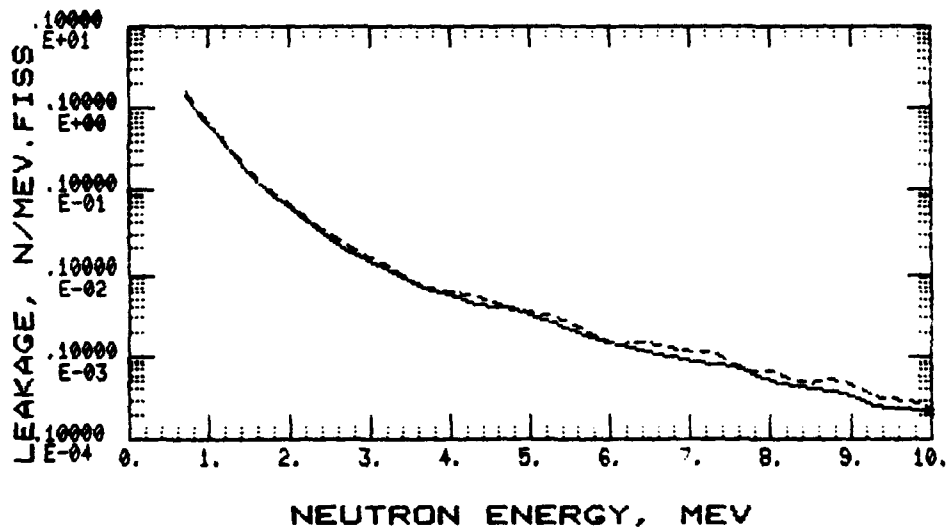


Figure 4 : Neutron spectra integrated over angle.

As is apparent the differences between 75-cm and 200-cm data are minor and correspond primarily to the previously-discussed increase in integral quantities of 11 %, as the source-to-detector separation is increased from 75 to 200 centimeters.

Boron-triflouride Detector Counting Data

Data recorded by the cadmium-covered boron-triflouride detector are shown in Table 3. These data cannot be directly transformed into fluence measurements without detailed knowledge of the neutron spectrum at each location, as the detector sensitivity varies approximately as the inverse of neutron velocity, in the range from 0.5 eV to 10 MeV. Because of this variation, the detector is most sensitive to low-energy neutrons (i.e. in the eV range) but insensitive to neutrons below 0.5 eV, as a result of the layer of cadmium surrounding the detector (of thickness equal to 1 mm). When appropriate calculated spectra become available they may be integrated against the energy-dependent counting efficiency (see Appendix C) and compared to the recorded data, as a further integral check on the calculation below the NE-213 lower threshold of 600 keV.

To correct approximately for the unknown backgrounds at 75 cm, three assumptions were employed and are compared in the table. The column labelled "Lower" results from the assumption that the backgrounds at the 75-cm positions are numerically equal to the foregrounds at 200 cm in the corresponding directions. This results in an over-estimate of the background contribution, and thus an underestimate of the actual counting rate. The column labelled "Net" results from the assumption that the backgrounds applicable at 75 cm are the same as measured at 200 cm. This assumption is the most realistic as it is fairly-confidently suspected that the fluence of room-return neutrons at the energies of greatest importance to BF_3 detector would not change significantly from 200 to 75 cm. The column labelled "Upper" results from the assumption that the backgrounds at 75 cm are identically zero - clearly an underestimation which results in a maximum upper limit for the derived counting rates.

In Table 3, the results of angular integration over $4\pi r^2$ of the BF_3 data indicates that the "Net" estimates determined for each radius differ by 19 %, the measurement at 200 cm being the higher of the two. This may be a valid difference (resulting from the differing obliquity of the source-detector geometries) or merely an artifact of the approximate method used to correct for the 75 cm background contribution. The "Upper" and "Lower" estimated bounds for the 75 cm data differ from the "Net" estimate by + 33 % and - 17 %, respectively. If these are considered to be the range of possible error in the 75-centimeter measurements, then the 200 cm measurements are consistent, and fall within these limits.

Cadmium-Covered BF_3 Counting Rates (counts/fission)

Angle (degrees)	Foreground			Background			Net Counting Rates		
	75 cm		200 cm	75 cm		200 cm	75 cm		200 cm
	Lower	Net	Upper	Lower	Net	Upper	Lower	Net	Upper
0.0	1.33-7	5.65-8	-	-	7.68-8	-	1.33-7	-	-
22.5	1.13-7	-	-	-	-	-	1.13-7	-	-
45.0	1.39-7	6.25-8	4.05-8	7.61-8	9.82-8	1.39-7	-	-	2.21-8
67.5	1.82-7	7.30-8	4.84-8	1.10-7	1.34-7	1.82-7	-	-	2.46-8
90.0	2.19-7	7.26-8	4.92-8	1.46-7	1.70-7	2.19-7	-	-	2.34-8
112.5	2.18-7	7.57-8	5.26-8	1.42-7	1.65-7	2.18-7	-	-	2.31-8
135.0	2.06-7	8.18-8	5.51-8	1.25-7	1.51-7	2.06-7	-	-	2.68-8
$4\pi r^2$	Integral (cm ² /fission) :			8.38-3	1.01-2	1.34-2	1.20-2	1.20-2	1.20-2

Table 3 : Cadmium-covered boron-trifluoride detector counting rates.

COMPARISON TO THEORETICAL CALCULATIONS

Two theoretical calculations are presently available for comparison to the measured neutron spectra. One was performed in 1976 [15] using a one-dimensional Monte-Carlo approximation and the other a two-dimensional calculation of 1982 [16], also using Monte-Carlo techniques. Both of these were intended to model the dynamically-disassembling weapon at Hiroshima rather than the zero yield experiment described herein, consequently differences were expected. In an actual detonation low energy neutrons are influenced both by the much higher temperature within the weapon and also its disassembly. High energy neutrons (such as monitored by the NE-213 detector) are less influenced by thermal effects, but do penetrate a casing reduced in density as a result of the explosion [8].

In Figures 5 and 6 comparisons are made between these two calculations (integrated over angle in the case of the 2-D results) and the DREO-measured spectra at 75 cm and 200 cm, respectively. For each measured spectrum three curves are shown, corresponding to the upper, lower and best estimates as predicted by the spectral unfolding procedure. The upper and lower estimates differ from the best estimate by amounts calculated to equal the expected standard deviation, based on counting statistics alone. Separate illustrations and tables for the angularly-integrated experimental results also appear in Appendices A and B.

The measured spectra fall below both sets of calculations, but are in better agreement with the more recent 2-D results. The spectral shape is, however, in very close agreement with both the 1976 and 1982 calculations. It is felt that the greater number of neutrons (above 600 keV) escaping from the weapon is due to the fact that at least some of the fast neutrons penetrate transport media reduced in density by the detonation, whereas there is no such reduction built into the COMET experimental assembly. Such a reduction in mean casing density would lead to an increase in neutron escape probability, especially at the time when the greatest numbers of neutrons were being produced (i.e. near the termination of the fission process). Comparison to calculations now underway at LANL will ultimately determine if this is indeed the cause of the noted differences.

Total neutron leakage between 0.64 and 10 MeV predicted by the 2-D calculation amounts to 0.0773 neutrons/fission. In comparison the measured leakage between these same energy limits was determined to equal 0.0586 at 75 cm and 0.0650 at 200 cm. The calculated value thus exceeds the measurement at 75 cm by 32 %, and the measurement at 200 cm by 19 %. As previously mentioned, total-leakage determinations are better performed at the farther distance due to the reduced magnitude of effective obliquity differences, consequently it is indicated that approximately 16 % fewer neutrons above 640 keV escape from the COMET casing.

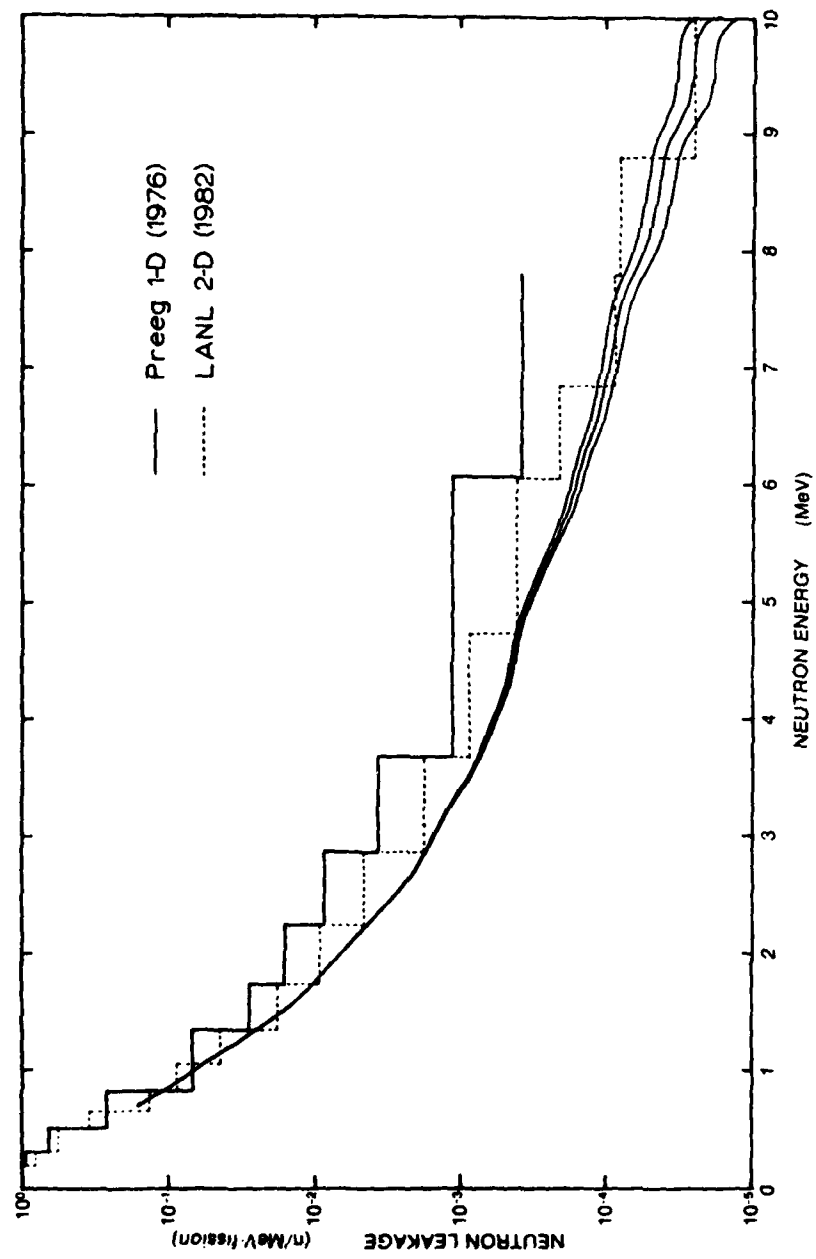


Figure 5 : Comparison of 75-cm leakage spectrum to calculations.

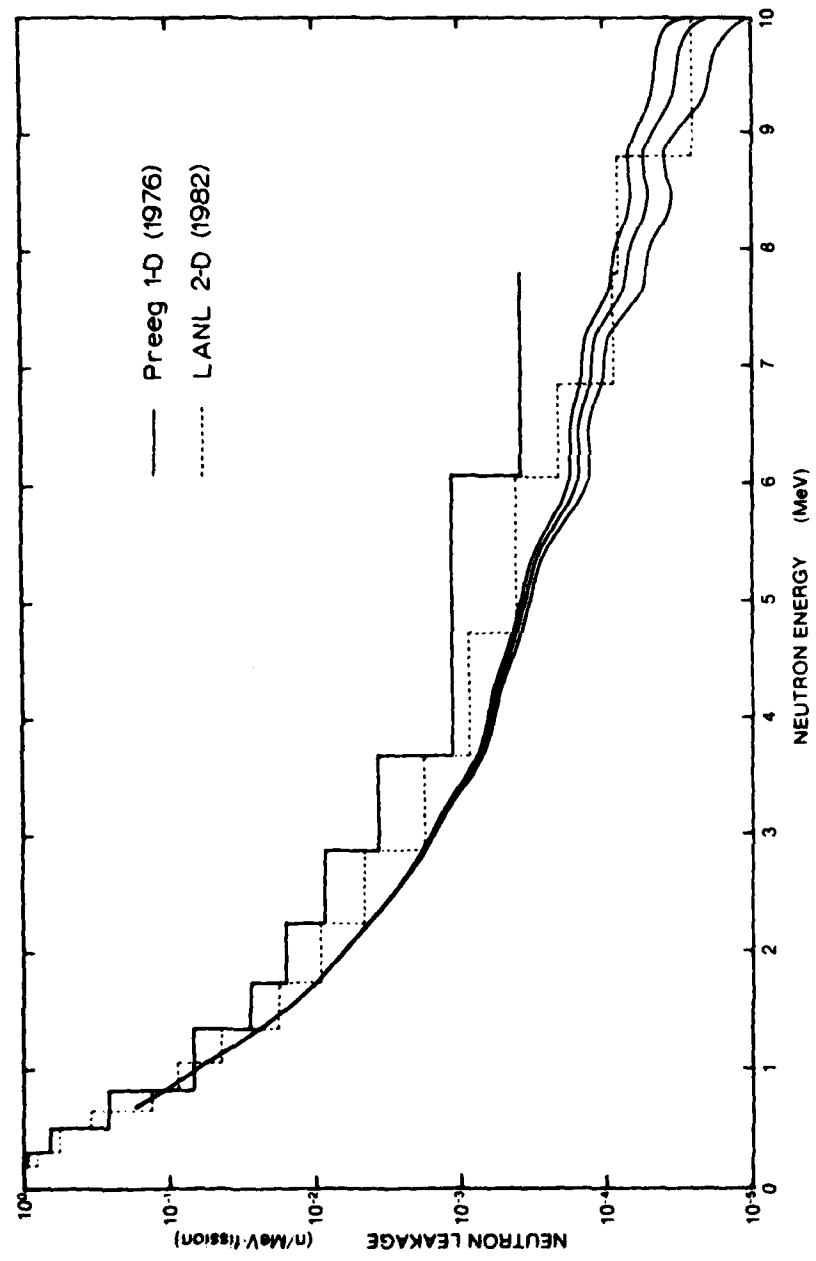


Figure 6 : Comparison of 200-cm leakage spectrum to calculations.

CONCLUSIONS

Neutron spectra above 600 keV have been measured in several directions surrounding the COMET assembly, and at two radii. Integration of the measurements over angle demonstrates that the spectra obtained at 75 cm are in good agreement and consistent with those measured at 200 cm. Comparison to theoretical calculations of the Hiroshima detonation indicates that the measurements are in very good agreement in spectral shape, but that slightly fewer fast neutrons leak from the COMET casing. Further calculations are required to fully verify this observation.

ACKNOWLEDGEMENTS

The authors are indebted to many of the staff of the Los Alamos National Laboratory for assistance in performing these measurements; in particular R.E. Malenfant and P.P. Whalen for program support, H.M. Forehand, G.E. Hansen and R. Pederson for operational and technical assistance and F.J. Muckenthaler (of ORNL) for many helpful suggestions.

REFERENCES

1. "Revised Dose Estimates at Hiroshima and Nagasaki"; W.E. Loewe and E. Mendelsohn; *Health Physics* Vol. 41, 663 (1981)
2. "Dosimetry of the Atomic Bomb Survivors"; W.K. Sinclair and P. Failla; *Radiation Research* Vol. 88, 437 (1981)
3. "Review of Dosimetry for the Atomic Bomb Survivors"; G.D. Kerr; *Fourth Symposium on Neutron Dosimetry*, Munich-Neuherberg (June, 1981)
4. "Reevaluation of Dosimetric Factors : Hiroshima and Nagasaki"; V.P. Bond and J.W. Thiessen (Eds.); U.S. Department of Energy Symposium Series 55, CONF-810928 (Sept 1981)
5. "Findings of a Recent ORNL Review of Dosimetry for the Japanese Atomic Bomb Survivors"; G.D. Kerr; *Oak Ridge National Laboratory Report ORNL/TM-8078* (1981)
6. "Neutron and Gamma-ray Doses at Hiroshima and Nagasaki"; W.E. Loewe and E. Mendelsohn; *Nuclear Science and Engineering* Vol. 81, 325 (1982)
7. "ICHIBAN : Radiation Dosimetry for the Survivors of the Bombings of Hiroshima and Nagasaki"; J.A. Auxier; *National Technical Information Service TID-27080* (1977)
8. "Status of Los Alamos Efforts Related to Hiroshima and Nagasaki Dose Estimates"; P.P. Whalen, in Ref. 4
9. "Rapid, On-line Matrix Unfolding of Fast-Neutron Spectroscopic Data from Organic Scintillators"; H.A. Robitaille; *Third Symposium on Neutron Dosimetry in Biology and Medicine*, Munich-Neuherberg, (May 1977)
10. "A Fast-Neutron Spectrometer"; F.P. Szabo; *Defence Research Establishment Ottawa Report R-637* (July, 1971)
11. "A Handbook of Radiation Shielding Data"; J.C. Courtney, Ed.; *Louisiana State University, ANS/SD-76/14* (July, 1976)
12. Memorandum from G.E. Hansen, Los Alamos National Laboratory, Q-2-83-3294A (11 Jan 83)
13. "Calculation of Neutron Fluence-to-Kerma Factors for the Human Body"; J.J. Ritts, M. Solomito and P.N. Stevens; *Nuclear Applications and Technology*, Vol 7, 89 (July 1969)
14. Annual Progress Report of the Health Physics Division; J.A. Auxier; *Oak Ridge National Laboratory ORNL-4446* (1969)

15. Letter to C.P. Knowles, R & D Associates; W.E. Preeg; LANL
(also published in ref 4, page 125)
16. "Source Terms for the Initial Radiations"; P.P. Whalen; Los
Alamos National Laboratory, LA-UR-83-198 (16 Feb 1983)

APPENDIX A : Plotted Neutron Spectra

On the following pages of this appendix are shown semi-logarithmic plots of the neutron spectra determined above 600 keV by the NE-213 detector, at each location of measurement. In all cases the data are normalized to fission rates as determined by LANL. Figures A-1 to A-7 illustrate the spectra measured at a source-to-detector separation of 75 cm, whereas Figures A-8 to A-13 illustrate those measurements performed at 200 cm. Figures A-14 and A-15 display the results of angular integration of the measured spectra at distances of 75cm and 200 cm, respectively.

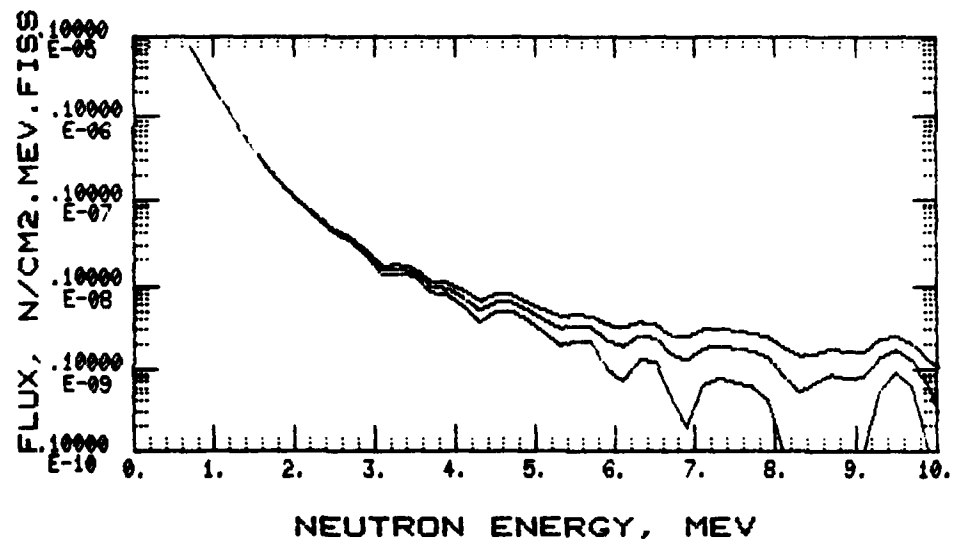


Figure A-1 : Neutron spectrum at 0 degrees and 75 cm.

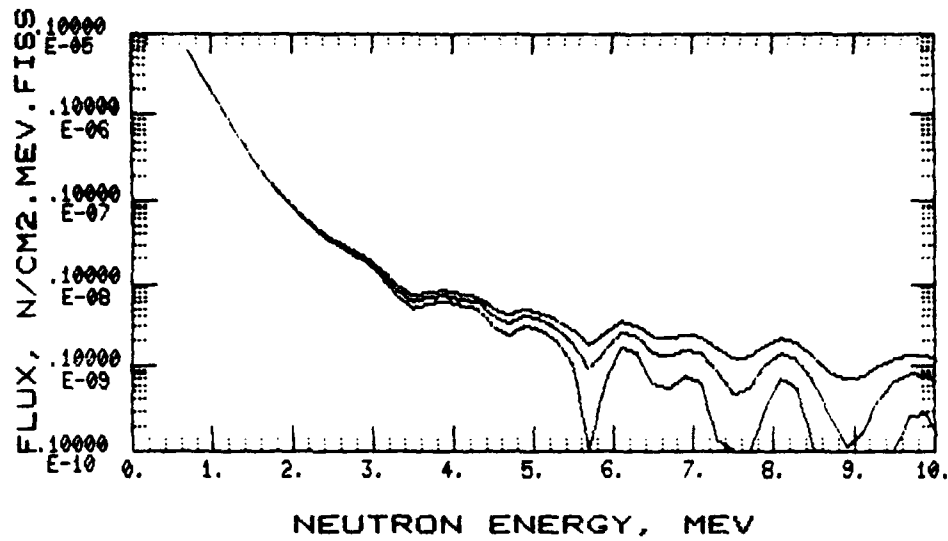


Figure A-2 : Neutron spectrum at 22.5 degrees and 75 cm.

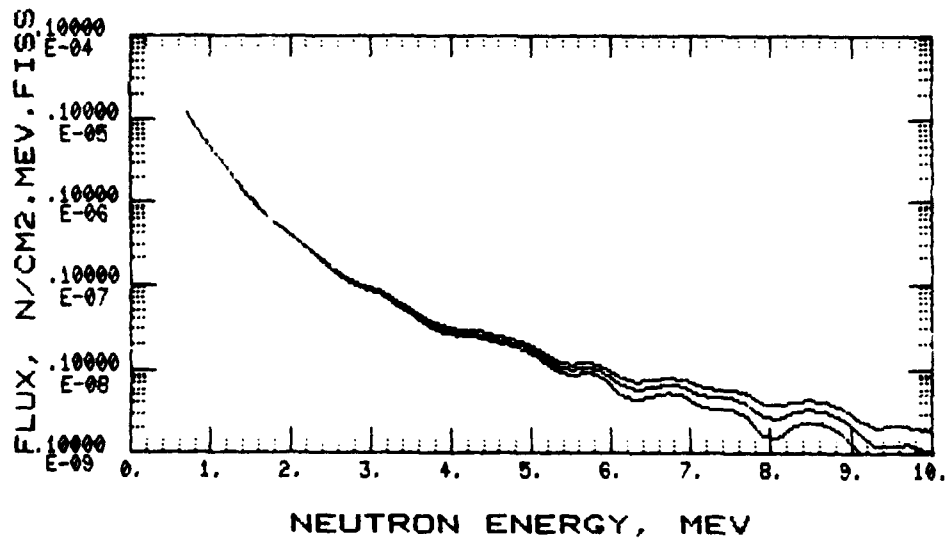


Figure A-3 : Neutron spectrum at 45 degrees and 75 cm.

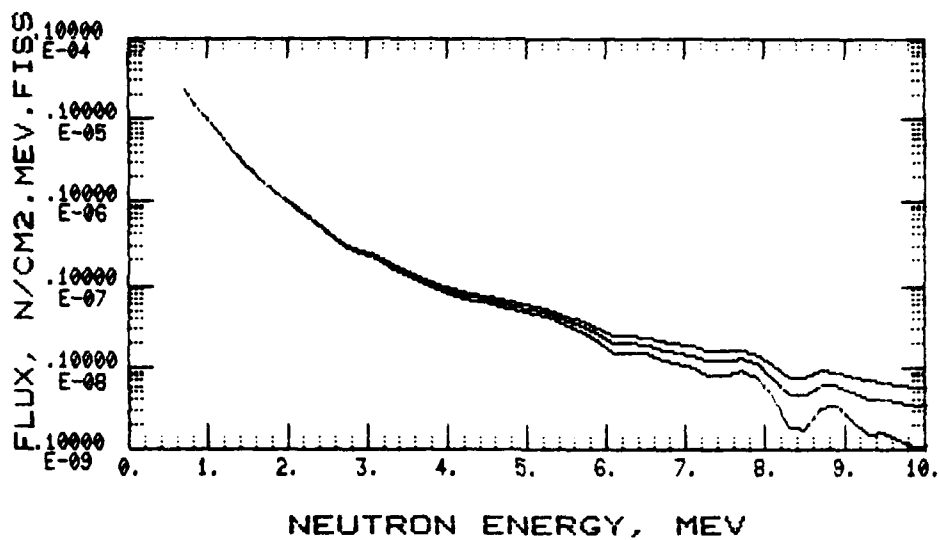


Figure A-4 : Neutron spectrum at 67.5 degrees and 75 cm.

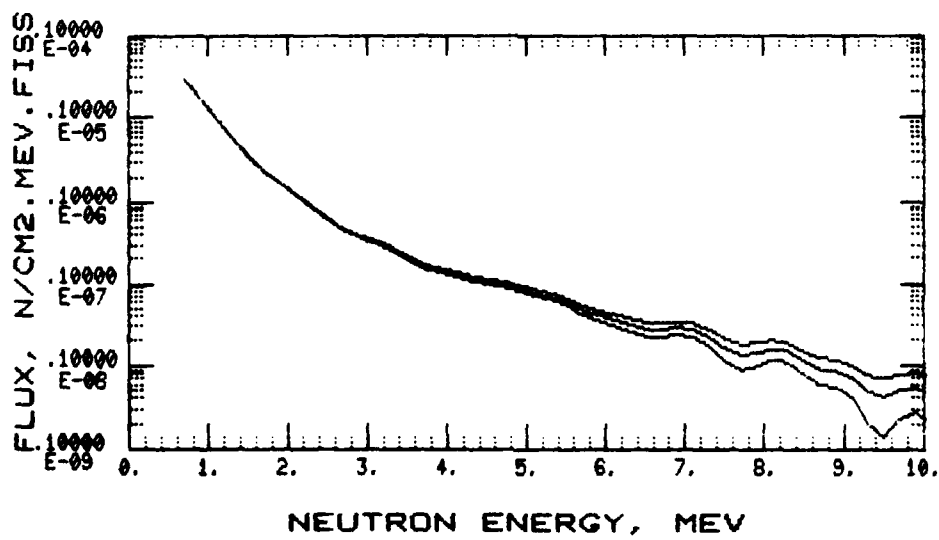


Figure A-5 : Neutron spectrum at 90 degrees and 75 cm.

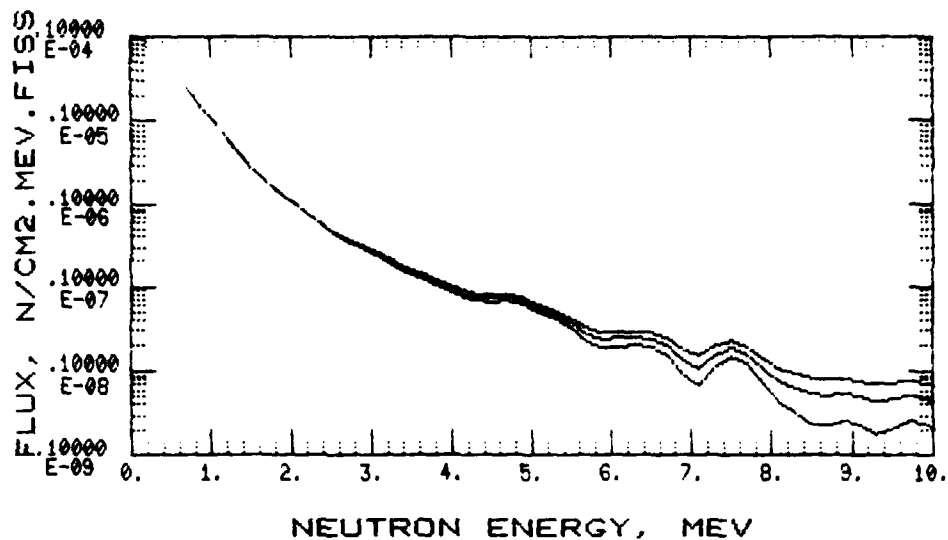


Figure A-6 : Neutron spectrum at 112.5 degrees and 75 cm.

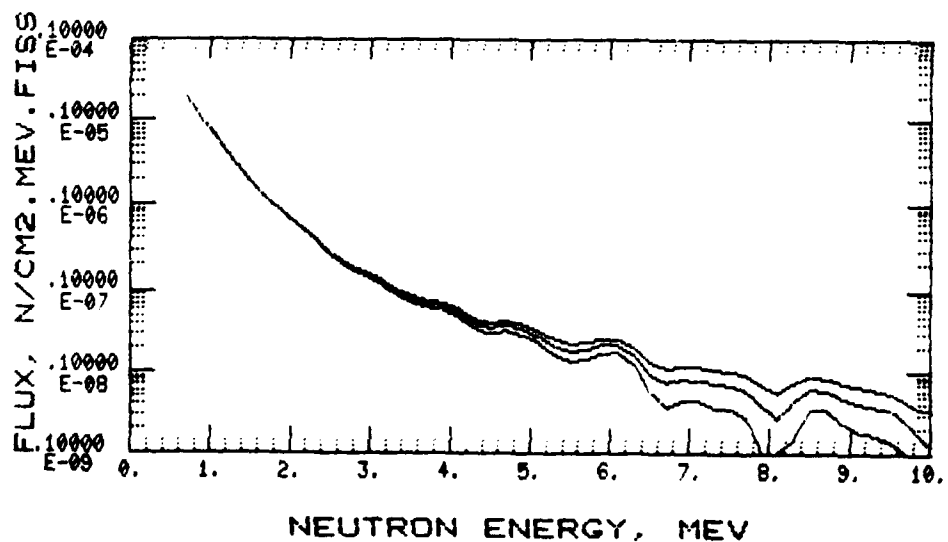


Figure A-7 : Neutron spectrum at 135 degrees and 75 cm.

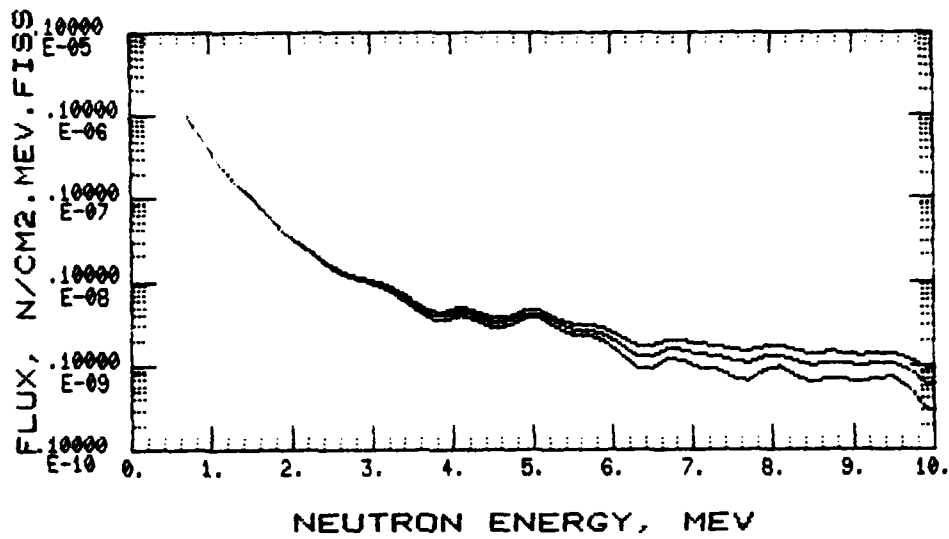


Figure A-8 : Neutron spectrum at 0 degrees and 200 cm.

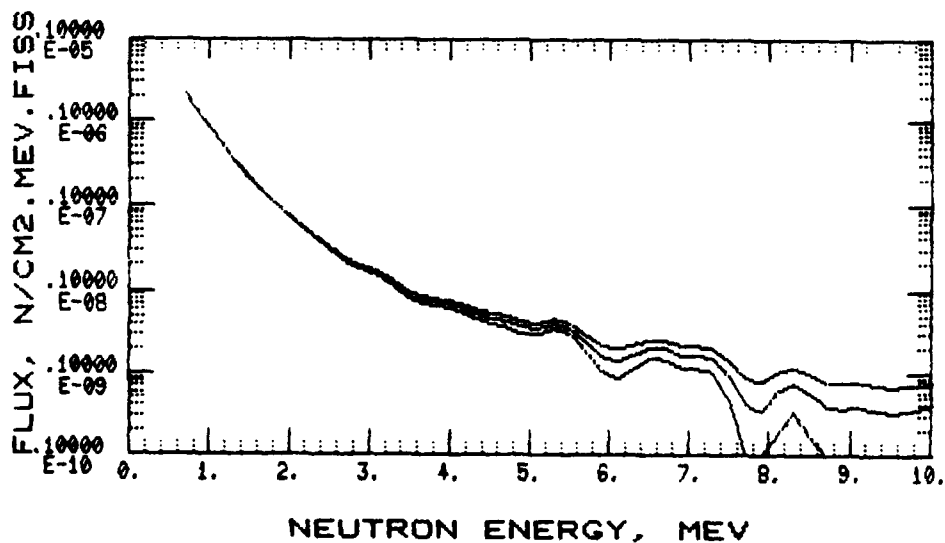


Figure A-9 : Neutron spectrum at 45 degrees and 200 cm.

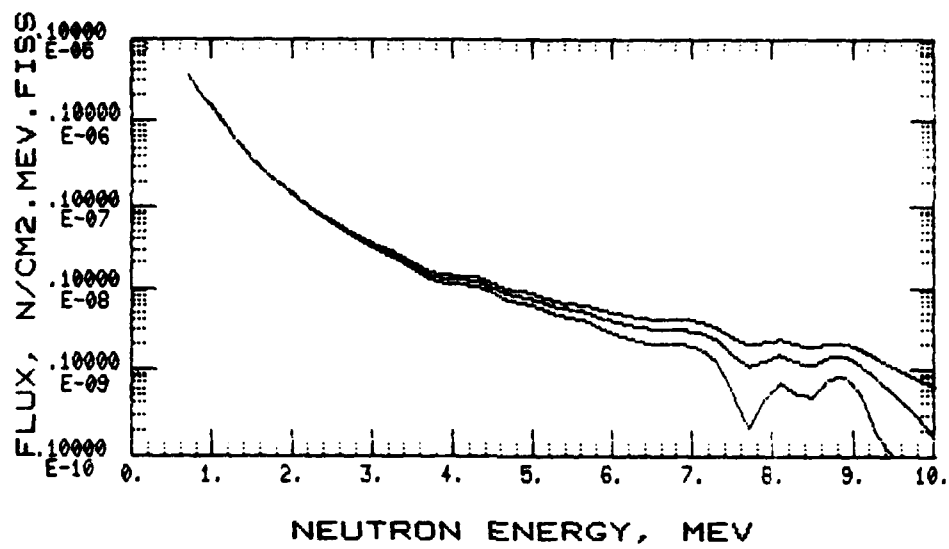


Figure A-10 : Neutron spectrum at 67.5 degrees and 200 cm.

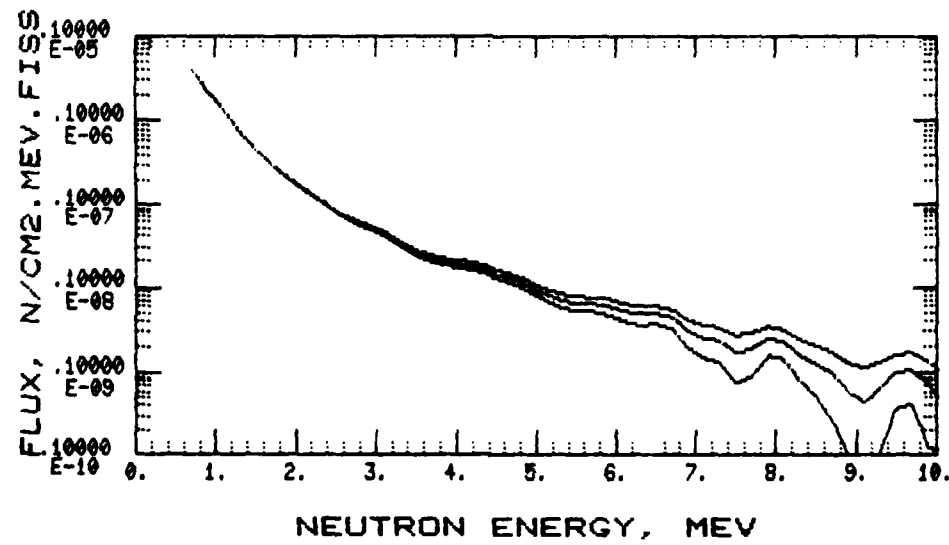


Figure A-11 : Neutron spectrum at 90 degrees and 200 cm.

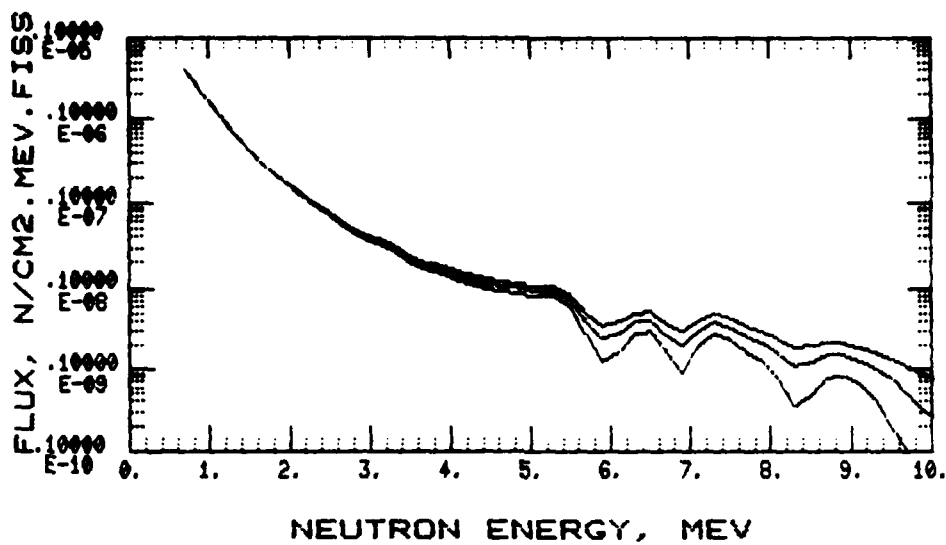


Figure A-12 : Neutron spectrum at 112.5 degrees and 200 cm.

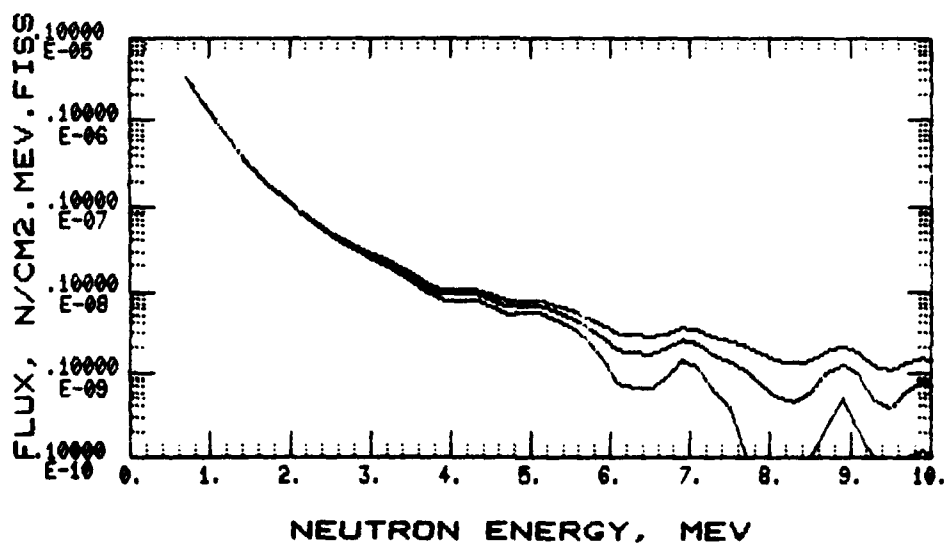


Figure A-13 : Neutron spectrum at 135 degrees and 200 cm.

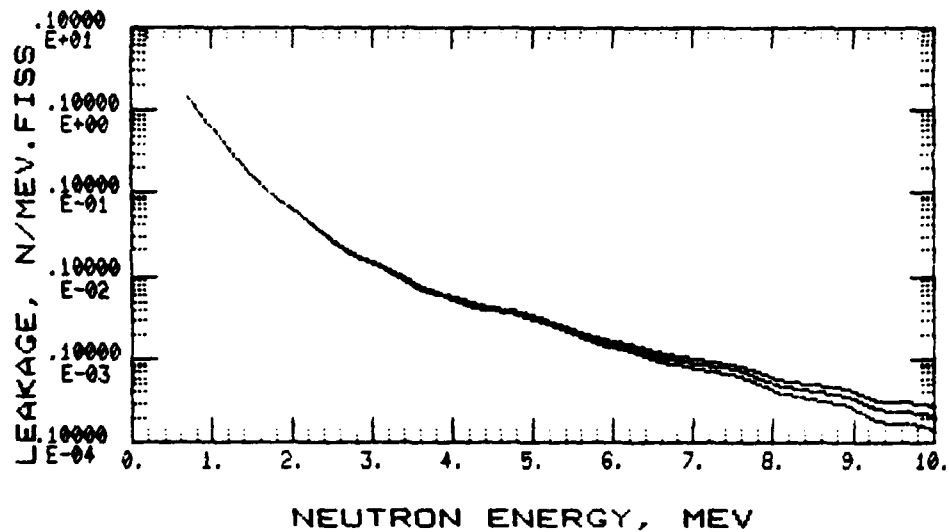


Figure A-14 : Neutron leakage spectrum at 75 cm.

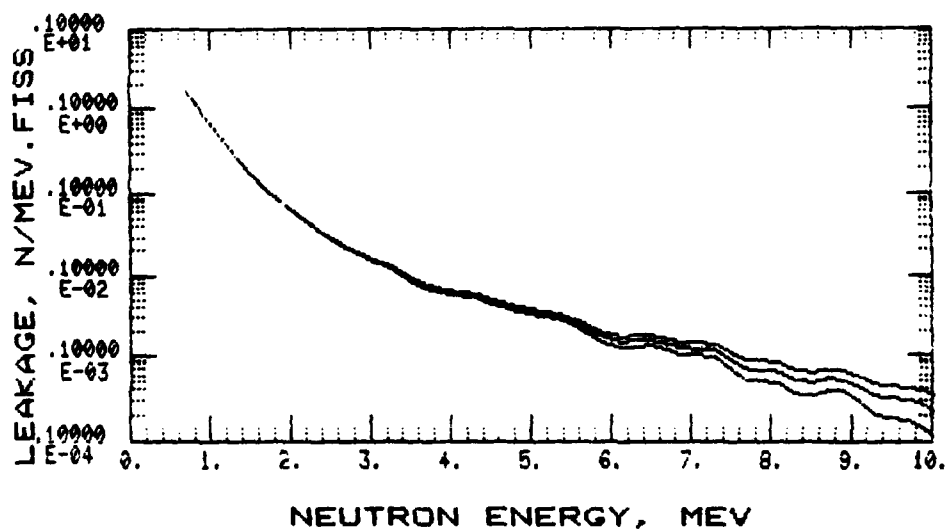


Figure A-15 : Neutron leakage spectrum at 200 cm.

APPENDIX B : Listed Neutron Spectra

Listed in Tables B-1 to B-15 are the neutron spectra corresponding to the illustrations in Appendix A. Tables B-1 to B-7 describe those measurements made at 75 cm, Tables B-8 to B-13 those at 200 cm, and Tables B-14 and B-15 the results of angular integrations of the measured spectra at 75 cm and 200 cm, respectively. The spectra are listed in bins of 200 keV width, from a lower energy of 600 keV up to a maximum of 10 MeV. Also listed are the statistical standard-errors estimated for each bin by the unfolding procedure. Note that these errors result from counting uncertainties only, and neglect systematic errors.

Table B-1

COMET NEUTRON SPECTRUM AT 0 DEG & 75 CM					
GROUP	UPPER ENERGY (REV)	PARTICLE FLUX (PARTICLES/CM2-NEV-FISS)	ERROR (STD. DEV.)	ERROR (%)	RUNNING INTEGRAL (/CM2-FISS)
1	0.8	6.716E-07	1.11E-09	0.17	1.332E-07
1.5	1.0	3.037E-07	5.33E-10	0.19	1.931E-07
2	1.2	1.433E-07	4.31E-10	0.30	2.237E-07
3	1.4	6.946E-08	3.36E-10	0.48	3.36E-07
4	1.6	3.198E-08	2.87E-10	0.82	2.446E-07
5	1.8	1.933E-08	2.42E-10	1.25	2.485E-07
6	2.0	1.172E-08	2.11E-10	1.79	2.508E-07
7	2.2	7.927E-09	1.90E-10	2.49	2.524E-07
8	2.4	5.362E-09	1.75E-10	3.25	2.535E-07
9	2.6	3.085E-09	1.61E-10	4.23	2.522E-07
10	2.8	3.042E-09	1.58E-10	5.19	2.548E-07
11	3.0	2.048E-09	1.61E-10	7.85	2.533E-07
12	3.2	1.333E-09	1.71E-10	12.81	2.555E-07
13	3.4	1.393E-09	1.59E-10	11.42	2.558E-07
14	3.6	1.276E-09	1.42E-10	11.11	2.561E-07
15	3.8	8.599E-10	1.35E-10	15.75	2.562E-07
16	4.0	8.108E-10	1.32E-10	16.35	2.564E-07
17	4.2	6.169E-10	1.37E-10	20.55	2.565E-07
18	4.4	4.458E-10	1.26E-10	28.40	2.566E-07
19	4.6	5.520E-10	1.25E-10	22.51	2.568E-07
20	4.8	5.571E-10	1.18E-10	21.06	2.568E-07
21	5.0	4.512E-10	1.11E-10	24.61	2.569E-07
22	5.2	3.554E-10	1.06E-10	30.71	2.570E-07
23	5.4	2.711E-10	1.04E-10	38.05	2.570E-07
24	5.6	2.920E-10	1.01E-10	34.55	2.571E-07
25	5.8	2.829E-10	1.00E-10	35.37	2.572E-07
26	6.0	1.936E-10	1.04E-10	53.27	2.572E-07
27	6.2	1.692E-10	1.05E-10	62.26	2.572E-07
28	6.4	2.161E-10	1.03E-10	47.40	2.573E-07
29	6.6	2.064E-10	9.56E-11	46.19	2.573E-07
30	6.8	2.920E-10	9.1E-11	70.81	2.574E-07
31	7.0	1.132E-10	9.74E-11	85.68	2.574E-07
32	7.2	1.564E-10	1.01E-10	64.58	2.574E-07
33	7.4	1.692E-10	1.01E-10	59.46	2.575E-07
34	7.6	1.551E-10	9.65E-11	62.18	2.575E-07
35	7.8	1.452E-10	9.21E-11	63.34	2.575E-07
36	8.0	1.201E-10	8.86E-11	71.60	2.575E-07
37	8.2	7.666E-11	8.38E-11	109.33	2.575E-07
38	8.4	4.52E-11	7.95E-11	172.97	2.575E-07
39	8.6	5.957E-11	7.82E-11	131.25	2.575E-07
40	8.8	7.611E-11	7.68E-11	101.01	2.575E-07
41	9.0	6.657E-11	7.31E-11	109.70	2.575E-07
42	9.2	7.374E-11	7.32E-11	99.32	2.576E-07
43	9.4	2.210E-10	7.48E-11	61.84	2.576E-07
44	9.6	1.518E-10	6.96E-11	45.86	2.576E-07
45	9.8	1.159E-10	6.14E-11	53.01	2.576E-07
46	10.0	5.516E-11	5.91E-11	107.13	2.577E-07

Table B-2

COMET NEUTRON SPECTRUM AT 22.5 DEG & 75 CM						
GROUP	UPPER ENERGY (MEV)	PARTICLE FLUX (PARTICLES/CM ² -MEV-FISS)	ERROR (STD. DEV.)	RUNNING INTEGRAL (CM ² -FISS)	ERROR (%)	RUNNING INTEGRAL (CM ² -FISS)
4	0.8	5.488E-07	9.04E-10	0.117	1.097E-07	4
5	1.0	2.504E-07	4.43E-10	0.118	1.598E-07	5
6	1.2	1.196E-07	3.31E-10	0.248	1.838E-07	6
7	1.4	5.720E-08	2.55E-10	0.455	1.952E-07	7
8	1.6	2.846E-08	2.16E-10	0.716	2.009E-07	8
9	1.8	1.542E-08	1.81E-10	1.171	2.039E-07	9
10	2.0	9.456E-09	1.55E-10	1.641	2.059E-07	10
11	2.2	6.005E-09	1.39E-10	2.311	2.071E-07	11
12	2.4	4.045E-09	1.27E-10	3.151	2.079E-07	12
13	2.6	2.850E-09	1.16E-10	4.071	2.084E-07	13
14	2.8	2.247E-09	1.14E-10	5.071	2.099E-07	14
15	3.0	1.746E-09	1.15E-10	6.581	2.092E-07	15
16	3.2	1.200E-09	1.18E-10	9.987	2.095E-07	16
17	3.4	7.446E-10	1.10E-10	14.715	2.096E-07	17
18	3.6	5.346E-10	1.03E-10	19.261	2.097E-07	18
19	3.8	6.070E-10	1.01E-10	16.571	2.098E-07	19
20	4.0	6.277E-10	9.74E-11	15.471	2.100E-07	20
21	4.2	5.549E-10	9.47E-11	17.091	2.101E-07	21
22	4.4	5.202E-10	9.12E-11	17.321	2.102E-07	22
23	4.6	3.496E-10	8.61E-11	24.631	2.103E-07	23
24	4.8	2.796E-10	8.40E-11	30.051	2.104E-07	24
25	5.0	3.532E-10	8.04E-11	22.741	2.104E-07	25
26	5.2	3.064E-10	7.57E-11	24.711	2.104E-07	26
27	5.4	2.365E-10	7.20E-11	30.461	2.105E-07	27
28	5.6	1.547E-10	6.91E-11	44.691	2.105E-07	28
29	5.8	8.118E-11	7.23E-11	88.011	2.105E-07	29
30	6.0	1.317E-10	7.75E-11	58.819	2.106E-07	30
31	6.2	2.221E-10	7.61E-11	34.281	2.106E-07	31
32	6.4	1.937E-10	7.04E-11	36.331	2.107E-07	32
33	6.6	1.215E-10	6.81E-11	56.041	2.107E-07	33
34	6.8	1.157E-10	6.91E-11	59.712	2.107E-07	34
35	7.0	1.356E-10	6.92E-11	51.031	2.107E-07	35
36	7.2	1.225E-10	6.76E-11	55.119	2.108E-07	36
37	7.4	7.675E-11	6.51E-11	84.861	2.108E-07	37
38	7.6	4.046E-11	6.45E-11	159.219	2.108E-07	38
39	7.8	4.857E-11	6.55E-11	134.814	2.108E-07	39
40	8.0	9.289E-11	6.46E-11	69.512	2.108E-07	40
41	8.2	1.235E-10	6.08E-11	49.119	2.109E-07	41
42	8.4	1.030E-10	5.55E-11	53.915	2.109E-07	42
43	8.6	5.714E-11	5.13E-11	89.818	2.109E-07	43
44	8.8	2.299E-11	5.03E-11	218.519	2.109E-07	44
45	9.0	9.500E-12	5.14E-11	540.815	2.109E-07	45
46	9.2	1.446E-11	5.18E-11	357.812	2.109E-07	46
47	9.4	3.361E-11	5.18E-11	153.912	2.109E-07	47
48	9.6	5.655E-11	5.10E-11	90.115	2.109E-07	48
49	9.8	7.048E-11	4.86E-11	68.915	2.109E-07	49
50	10.0	6.909E-11	4.49E-11	65.041	2.110E-07	50

Table B-3

COMET NEUTRON SPECTRUM AT 45 DEG & 75 CM						
GROUP	UPPER ENERGY (MEV)	PARTICLE FLUX (PARTICLES/CM ² -MEV-FISS)	ERROR (STD. DEV.)	UPPER ENERGY (MEV)	PARTICLE FLUX (PARTICLES/CM ² -MEV-FISS)	ERROR (%)
4	0.8	5.488E-07	9.04E-10	0.117	1.097E-07	4
5	1.0	2.504E-07	4.43E-10	0.118	1.598E-07	5
6	1.2	1.196E-07	3.31E-10	0.248	1.838E-07	6
7	1.4	5.720E-08	2.55E-10	0.455	1.952E-07	7
8	1.6	2.846E-08	2.16E-10	0.716	2.009E-07	8
9	1.8	1.542E-08	1.81E-10	1.171	2.039E-07	9
10	2.0	9.456E-09	1.55E-10	1.641	2.059E-07	10
11	2.2	6.005E-09	1.39E-10	2.311	2.071E-07	11
12	2.4	4.045E-09	1.27E-10	3.151	2.079E-07	12
13	2.6	2.850E-09	1.16E-10	4.071	2.084E-07	13
14	2.8	2.247E-09	1.14E-10	5.071	2.099E-07	14
15	3.0	1.746E-09	1.15E-10	6.581	2.092E-07	15
16	3.2	1.200E-09	1.18E-10	9.987	2.095E-07	16
17	3.4	7.446E-10	1.10E-10	14.715	2.096E-07	17
18	3.6	5.346E-10	1.03E-10	19.261	2.097E-07	18
19	3.8	6.070E-10	1.01E-10	16.571	2.098E-07	19
20	4.0	6.277E-10	9.74E-11	15.471	2.100E-07	20
21	4.2	5.549E-10	9.47E-11	17.091	2.101E-07	21
22	4.4	5.202E-10	9.12E-11	17.321	2.102E-07	22
23	4.6	3.496E-10	8.61E-11	24.631	2.103E-07	23
24	4.8	2.796E-10	8.40E-11	30.051	2.104E-07	24
25	5.0	3.532E-10	8.04E-11	22.741	2.104E-07	25
26	5.2	3.064E-10	7.57E-11	24.711	2.104E-07	26
27	5.4	2.365E-10	7.20E-11	30.461	2.105E-07	27
28	5.6	1.547E-10	6.91E-11	44.691	2.105E-07	28
29	5.8	8.118E-11	7.23E-11	88.011	2.105E-07	29
30	6.0	1.317E-10	7.75E-11	58.819	2.106E-07	30
31	6.2	2.221E-10	7.61E-11	34.281	2.106E-07	31
32	6.4	1.937E-10	7.04E-11	36.331	2.107E-07	32
33	6.6	1.215E-10	6.81E-11	56.041	2.107E-07	33
34	6.8	1.157E-10	6.91E-11	59.712	2.107E-07	34
35	7.0	1.356E-10	6.92E-11	51.031	2.107E-07	35
36	7.2	1.225E-10	6.76E-11	55.119	2.108E-07	36
37	7.4	7.675E-11	6.51E-11	84.861	2.108E-07	37
38	7.6	4.046E-11	6.45E-11	159.219	2.108E-07	38
39	7.8	4.857E-11	6.55E-11	134.814	2.108E-07	39
40	8.0	9.289E-11	6.46E-11	69.512	2.108E-07	40
41	8.2	1.235E-10	6.08E-11	49.119	2.109E-07	41
42	8.4	1.030E-10	5.55E-11	53.915	2.109E-07	42
43	8.6	5.714E-11	5.13E-11	89.818	2.109E-07	43
44	8.8	2.299E-11	5.03E-11	218.519	2.109E-07	44
45	9.0	9.500E-12	5.14E-11	540.815	2.109E-07	45
46	9.2	1.446E-11	5.18E-11	357.812	2.109E-07	46
47	9.4	3.361E-11	5.18E-11	153.912	2.109E-07	47
48	9.6	5.655E-11	5.10E-11	90.115	2.109E-07	48
49	9.8	7.048E-11	4.86E-11	68.915	2.109E-07	49
50	10.0	6.909E-11	4.49E-11	65.041	2.110E-07	50

COMET NEUTRON SPECTRUM AT 45 DEG & 75 CM

GROUP (MEV)

UPPER ENERGY (MEV)

PARTICLE FLUX (PARTICLES/CM²-MEV-FISS)

ERROR (STD. DEV.)

PARTICLE FLUX (PARTICLES/CM²-MEV-FISS)

ERROR (%)

COMET NEUTRON SPECTRUM AT 45 DEG & 75 CM

GROUP (MEV)

UPPER ENERGY (MEV)

PARTICLE FLUX (PARTICLES/CM²-MEV-FISS)

ERROR (STD. DEV.)

PARTICLE FLUX (PARTICLES/CM²-MEV-FISS)

ERROR (%)

Table B-4

COMET NEUTRON SPECTRUM AT 67.5 DEG & 75 CM						COMET NEUTRON SPECTRUM AT 90 DEG & 75 CM					
GROUP	UPPER ENERGY (MEV)	PARTICLE FLUX (PARTICLES/CM ² -MEV-FISS.)	ERROR (STD.)	ERROR (%)	RUNNING INTEGRAL (/CM ² -MEV-FISS.)	GROUP	UPPER ENERGY (MEV)	PARTICLE FLUX (PARTICLES/CM ² -MEV-FISS.)	ERROR (STD.)	ERROR (%)	RUNNING INTEGRAL (/CM ² -FISS.)
4	0.8	2.019E-06	3.89E-09	0.19	4.039E-07	4	0.8	2.519E-06	5.03E-09	0.20	5.039E-07
5	1.0	1.144E-06	1.85E-09	0.16	6.328E-07	5	1.0	1.476E-06	2.38E-09	0.16	7.991E-07
6	1.2	6.751E-07	1.49E-09	0.22	7.670E-07	6	1.2	9.009E-07	1.76E-09	0.20	9.789E-07
7	1.4	3.791E-07	1.26E-09	0.23	8.433E-07	7	1.4	5.185E-07	1.51E-09	0.29	1.083E-06
8	1.6	2.204E-07	1.17E-09	0.53	8.877E-07	8	1.6	3.105E-07	1.40E-09	0.45	1.146E-06
9	1.8	1.451E-07	1.04E-09	0.72	9.167E-07	9	1.8	2.068E-07	1.26E-09	0.61	1.187E-06
10	2.0	1.023E-07	9.30E-10	0.91	9.368E-07	10	2.0	1.504E-07	1.14E-09	0.76	1.277E-06
11	2.2	7.449E-08	8.54E-10	1.15	9.510E-07	11	2.2	1.105E-07	1.04E-09	0.95	1.239E-06
12	2.4	5.339E-08	7.92E-10	1.48	9.632E-07	12	2.4	7.900E-08	9.44E-10	1.22	1.254E-06
13	2.6	3.722E-08	7.28E-10	1.95	9.702E-07	13	2.6	5.636E-08	8.95E-10	1.59	1.266E-06
14	2.8	2.639E-08	7.30E-10	2.76	9.754E-07	14	2.8	4.157E-08	8.95E-10	2.16	1.275E-06
15	3.0	2.161E-08	7.64E-10	3.53	9.798E-07	15	3.0	3.365E-08	9.39E-10	2.78	1.291E-06
16	3.2	1.892E-08	7.97E-10	4.21	9.833E-07	16	3.2	2.823E-08	9.82E-10	3.47	1.287E-06
17	3.4	1.525E-08	7.28E-10	4.78	9.868E-07	17	3.4	2.360E-08	8.95E-10	3.79	1.291E-06
18	3.6	1.228E-08	6.61E-10	5.38	9.895E-07	18	3.6	1.801E-08	8.11E-10	4.50	1.255E-06
19	3.8	1.011E-08	6.30E-10	6.23	9.912E-07	19	3.8	1.430E-08	7.79E-10	5.45	1.298E-06
20	4.0	8.412E-09	6.11E-10	7.26	9.930E-07	20	4.0	1.212E-08	7.39E-10	5.88	1.300E-06
21	4.2	7.096E-09	5.96E-10	8.41	9.939E-07	21	4.2	1.152E-08	7.40E-10	6.43	1.303E-06
22	4.4	6.324E-09	5.83E-10	9.23	9.956E-07	22	4.4	1.005E-08	7.21E-10	7.18	1.304E-06
23	4.6	6.096E-09	5.54E-10	9.10	9.965E-07	23	4.6	9.299E-09	6.87E-10	7.45	1.306E-06
24	4.8	5.412E-09	5.22E-10	9.64	9.974E-07	24	4.8	8.545E-09	6.47E-10	7.58	1.308E-06
25	5.0	4.814E-09	4.93E-10	10.24	9.994E-07	25	5.0	7.656E-09	6.9E-10	7.95	1.310E-06
26	5.2	4.500E-09	4.63E-10	10.30	1.000E-06	26	5.2	6.664E-09	5.74E-10	8.61	1.311E-06
27	5.4	3.982E-09	4.34E-10	10.90	1.000E-06	27	5.4	6.044E-09	5.41E-10	9.00	1.312E-06
28	5.6	3.282E-09	4.15E-10	12.63	1.000E-06	28	5.6	5.28E-09	5.15E-10	7.75	1.313E-06
29	5.8	2.850E-09	4.16E-10	14.60	1.002E-06	29	5.8	4.209E-09	5.17E-10	12.26	1.314E-06
30	6.0	2.239E-09	4.19E-10	18.71	1.002E-06	30	6.0	3.922E-09	5.55E-10	15.05	1.315E-06
31	6.2	1.730E-09	4.10E-10	23.70	1.003E-06	31	6.2	3.131E-09	5.09E-10	16.26	1.316E-06
32	6.4	1.711E-09	3.94E-10	23.02	1.003E-06	32	6.4	2.682E-09	4.85E-10	18.07	1.311E-06
33	6.6	1.668E-09	3.79E-10	22.63	1.004E-06	33	6.6	2.375E-09	4.67E-10	19.66	1.317E-06
34	6.8	1.469E-09	3.68E-10	25.11	1.004E-06	34	6.8	2.352E-09	4.57E-10	19.45	1.319E-06
35	7.0	1.354E-09	3.63E-10	26.84	1.004E-06	35	7.0	2.435E-09	4.48E-10	18.40	1.318E-06
36	7.2	1.244E-09	3.58E-10	28.81	1.004E-06	36	7.2	2.361E-09	4.35E-10	18.42	1.318E-06
37	7.4	1.070E-09	3.53E-10	32.96	1.004E-06	37	7.4	1.931E-09	4.19E-10	21.70	1.318E-06
38	7.6	1.118E-09	3.41E-10	32.47	1.004E-06	38	7.6	1.411E-09	4.05E-10	28.35	1.318E-06
39	7.8	1.120E-09	3.22E-10	28.66	1.004E-06	39	7.8	1.164E-09	3.82E-10	32.86	1.319E-06
40	8.0	9.833E-10	3.03E-10	30.34	1.004E-06	40	8.0	1.222E-09	3.65E-10	29.88	1.319E-06
41	8.2	6.696E-10	2.79E-10	41.60	1.000E-06	41	8.2	1.333E-09	3.43E-10	24.97	1.319E-06
42	8.4	4.248E-10	2.64E-10	62.25	1.005E-06	42	8.4	1.296E-09	3.18E-10	24.51	1.319E-06
43	8.6	4.119E-10	2.61E-10	63.31	1.005E-06	43	8.6	9.866E-10	2.98E-10	30.21	1.320E-06
44	8.8	5.389E-10	2.59E-10	48.07	1.005E-06	44	8.8	7.942E-10	2.86E-10	35.96	1.320E-06
45	9.0	5.466E-10	2.50E-10	45.76	1.005E-06	45	9.0	7.536E-10	2.71E-10	36.02	1.320E-06
46	9.2	4.296E-10	2.42E-10	56.35	1.005E-06	46	9.2	6.159E-10	2.55E-10	41.50	1.320E-06
47	9.4	3.693E-10	2.36E-10	64.01	1.005E-06	47	9.4	4.192E-10	2.46E-10	58.74	1.320E-06
48	9.6	3.623E-10	2.25E-10	62.19	1.005E-06	48	9.6	3.661E-10	2.35E-10	66.97	1.320E-06
49	9.8	3.271E-10	2.17E-10	66.11	1.005E-06	49	9.8	4.43E-10	2.44E-10	54.90	1.320E-06
50	10.0	3.039E-10	2.15E-10	70.63	1.005E-06	50	10.0	4.736E-10	2.35E-10	49.62	1.321E-06

Table B-5

Table B-6

GROUP	UPPER ENERGY (MEV)	PARTICLE FLUX (PARTICLES/CM ² -MEV-FISS)	ERROR (%)	RUNNING INTEGRAL (/CM ² -FISS)	GROUP	UPPER ENERGY (MEV)	PARTICLE FLUX (PARTICLES/CM ² -MEV-FISS)	ERROR (%)	RUNNING INTEGRAL (/CM ² -FISS)	
4	0.8	2.220E-06	4.31E-09	0.19	4.440E-07	4	0.8	1.714E-06	3.26E-09	3.427E-07
5	1.0	1.268E-06	2.1E-09	0.16	6.97E-07	5	1.0	9.272E-07	9.27E-09	5.282E-07
6	1.2	7.541E-07	1.57E-09	0.21	8.483E-07	6	1.2	5.207E-07	1.42E-09	6.323E-07
7	1.4	4.234E-07	1.32E-09	0.31	9.333E-07	7	1.4	2.804E-07	1.18E-09	6.883E-07
8	1.6	2.179E-07	1.22E-09	0.49	9.852E-07	8	1.6	1.582E-07	1.07E-09	7.200E-07
9	1.8	1.638E-07	1.09E-09	0.66	1.015E-06	9	1.8	9.982E-08	9.47E-10	7.399E-07
10	2.0	1.154E-07	9.4E-10	0.85	1.019E-06	10	2.0	6.978E-08	8.42E-10	7.539E-07
11	2.2	8.303E-08	8.35E-10	1.07	1.05E-06	11	2.2	5.011E-08	7.61E-10	4.52
12	2.4	5.892E-08	8.27E-10	1.40	1.06E-06	12	2.4	3.490E-08	6.98E-10	2.00
13	2.6	4.168E-08	7.62E-10	1.83	1.075E-06	13	2.6	2.331E-08	6.39E-10	2.74
14	2.8	3.170E-08	7.61E-10	2.40	1.082E-06	14	2.8	1.718E-08	6.39E-10	7.790E-07
15	3.0	2.568E-08	7.55E-10	3.06	1.087E-06	15	3.0	1.416E-08	6.61E-10	3.72
16	3.2	2.083E-08	8.15E-10	3.91	1.090E-06	16	3.2	1.146E-08	6.85E-10	4.67
17	3.4	1.634E-08	7.45E-10	4.56	1.094E-06	17	3.4	8.723E-09	6.27E-10	7.19
18	3.6	1.305E-08	6.77E-10	5.18	1.096E-06	18	3.6	6.941E-09	5.72E-10	8.23
19	3.8	1.108E-08	6.44E-10	5.82	1.099E-06	19	3.8	6.106E-09	5.46E-10	8.94
20	4.0	9.088E-09	6.23E-10	6.85	1.101E-06	20	4.0	5.668E-09	5.26E-10	9.28
21	4.2	7.392E-09	6.10E-10	6.24	1.102E-06	21	4.2	4.679E-09	4.07E-10	7.905E-07
22	4.4	6.556E-09	5.96E-10	9.09	1.104E-06	22	4.4	3.482E-09	4.94E-10	14.18
23	4.6	6.341E-09	5.95E-10	8.98	1.104E-06	23	4.6	3.104E-09	4.75E-10	15.33
24	4.8	6.465E-09	6.35E-10	8.28	1.106E-06	24	4.8	3.272E-09	4.51E-10	7.925E-07
25	5.0	5.836E-09	4.97E-10	8.51	1.107E-06	25	5.0	2.949E-09	4.23E-10	14.33
26	5.2	4.30E-09	4.65E-10	9.83	1.108E-06	26	5.2	2.345E-09	3.98E-10	16.99
27	5.4	3.939E-09	4.38E-10	11.12	1.109E-06	27	5.4	1.789E-09	3.79E-10	7.939E-07
28	5.6	3.161E-09	4.20E-10	13.28	1.110E-06	28	5.6	1.548E-09	3.70E-10	23.90
29	5.8	2.369E-09	4.26E-10	17.99	1.110E-06	29	5.8	1.619E-09	3.77E-10	7.942E-07
30	6.0	2.025E-09	4.39E-10	21.64	1.111E-06	30	6.0	1.816E-09	3.82E-10	21.00
31	6.2	2.090E-09	4.29E-10	20.52	1.111E-06	31	6.2	1.857E-09	3.60E-10	19.35
32	6.4	2.144E-09	4.09E-10	19.07	1.111E-06	32	6.4	1.402E-09	3.31E-10	21.58
33	6.6	2.031E-09	3.89E-10	19.18	1.111E-06	33	6.6	8.188E-10	3.17E-10	38.63
34	6.8	1.722E-09	3.75E-10	21.52	1.112E-06	34	6.8	6.409E-10	3.16E-10	7.958E-07
35	7.0	1.180E-09	3.69E-10	31.33	1.112E-06	35	7.0	6.973E-10	3.15E-10	45.15
36	7.2	9.728E-10	3.73E-10	38.32	1.112E-06	36	7.2	6.931E-10	3.12E-10	45.06
37	7.4	1.363E-09	3.70E-10	27.15	1.113E-06	37	7.4	6.309E-10	3.06E-10	7.963E-07
38	7.6	1.639E-09	3.48E-10	21.22	1.113E-06	38	7.6	5.928E-10	2.95E-10	49.67
39	7.8	1.375E-09	3.19E-10	23.24	1.113E-06	39	7.8	5.183E-10	2.80E-10	53.92
40	8.0	9.149E-10	2.98E-10	32.61	1.113E-06	40	8.0	3.287E-10	2.64E-10	7.966E-07
41	8.2	6.497E-10	2.85E-10	43.93	1.114E-06	41	8.2	2.293E-10	2.60E-10	113.21
42	8.4	5.516E-10	2.75E-10	49.95	1.114E-06	42	8.4	3.799E-10	2.56E-10	7.967E-07
43	8.6	4.692E-10	2.68E-10	57.03	1.114E-06	43	8.6	5.422E-10	2.40E-10	44.39
44	8.8	4.521E-10	2.61E-10	57.99	1.114E-06	44	8.8	5.146E-10	2.25E-10	43.66
45	9.0	4.768E-10	2.51E-10	52.62	1.114E-06	45	9.0	4.185E-10	2.17E-10	51.84
46	9.2	4.315E-10	2.37E-10	54.89	1.114E-06	46	9.2	3.589E-10	2.07E-10	57.76
47	9.4	3.807E-10	2.32E-10	60.88	1.114E-06	47	9.4	3.354E-10	1.96E-10	58.46
48	9.6	4.055E-10	2.32E-10	57.32	1.114E-06	48	9.6	3.004E-10	1.82E-10	7.971E-07
49	9.8	4.470E-10	2.28E-10	50.99	1.114E-06	49	9.8	2.119E-10	1.69E-10	80.07
50	10.0	4.282E-10	2.18E-10	51.05	1.114E-06	50	10.0	1.258E-10	1.71E-10	135.94

Table B-7

COMET NEUTRON SPECTRUM AT 135 DEG & 75 CM										
GROUP	UPPER ENERGY (MEV)	PARTICLE FLUX (PARTICLES/CM ² -MEV-FISS)	ERROR (%)	RUNNING INTEGRAL (/CM ² -FISS)	GROUP	UPPER ENERGY (MEV)	PARTICLE FLUX (PARTICLES/CM ² -MEV-FISS)	ERROR (%)	RUNNING INTEGRAL (/CM ² -FISS)	
4	0.8	2.220E-06	4.31E-09	0.19	4.440E-07	4	0.8	1.714E-06	3.26E-09	0.19
5	1.0	1.268E-06	2.1E-09	0.16	6.97E-07	5	1.0	9.272E-07	9.27E-09	0.21
6	1.2	7.541E-07	1.57E-09	0.21	8.483E-07	6	1.2	5.207E-07	1.42E-09	0.21
7	1.4	4.234E-07	1.32E-09	0.31	9.333E-07	7	1.4	2.804E-07	1.18E-09	0.42
8	1.6	2.179E-07	1.22E-09	0.49	9.852E-07	8	1.6	1.582E-07	1.07E-09	0.47
9	1.8	1.638E-07	1.09E-09	0.66	1.015E-06	9	1.8	9.982E-08	9.47E-10	0.95
10	2.0	1.154E-07	9.4E-10	0.85	1.019E-06	10	2.0	6.978E-08	8.42E-10	1.21
11	2.2	8.303E-08	8.35E-10	1.07	1.05E-06	11	2.2	5.011E-08	7.61E-10	1.52
12	2.4	5.892E-08	8.27E-10	1.40	1.06E-06	12	2.4	3.490E-08	6.98E-10	2.00
13	2.6	4.168E-08	7.62E-10	1.83	1.075E-06	13	2.6	2.331E-08	6.39E-10	2.74
14	2.8	3.170E-08	7.61E-10	2.40	1.082E-06	14	2.8	1.718E-08	6.39E-10	3.72
15	3.0	2.568E-08	7.55E-10	3.06	1.087E-06	15	3.0	1.416E-08	6.61E-10	4.67
16	3.2	2.083E-08	8.15E-10	3.91	1.090E-06	16	3.2	1.146E-08	6.85E-10	7.84E-07
17	3.4	1.634E-08	7.45E-10	4.56	1.094E-06	17	3.4	8.723E-09	6.27E-10	7.859E-07
18	3.6	1.305E-08	6.77E-10	5.18	1.096E-06	18	3.6	6.941E-09	5.72E-10	8.23
19	3.8	1.108E-08	6.44E-10	5.82	1.099E-06	19	3.8	6.106E-09	5.46E-10	8.94
20	4.0	9.088E-09	6.23E-10	6.85	1.101E-06	20	4.0	5.668E-09	5.26E-10	9.28
21	4.2	7.392E-09	6.10E-10	6.24	1.102E-06	21	4.2	4.679E-09	4.07E-10	7.905E-07
22	4.4	6.556E-09	5.96E-10	9.09	1.104E-06	22	4.4	3.482E-09	4.94E-10	14.18
23	4.6	6.341E-09	5.95E-10	8.98	1.104E-06	23	4.6	3.104E-09	4.75E-10	15.33
24	4.8	6.465E-09	6.35E-10	8.28	1.106E-06	24	4.8	3.272E-09	4.51E-10	7.925E-07
25	5.0	5.836E-09	4.97E-10	8.51	1.107E-06	25	5.0	2.949E-09	4.23E-10	14.33
26	5.2	4.30E-09	4.65E-10	9.83	1.108E-06	26	5.2	2.345E-09	3.98E-10	7.936E-07
27	5.4	3.939E-09	4.38E-10	11.12	1.109E-06	27	5.4	1.789E-09	3.79E-10	21.17
28	5.6	3.161E-09	4.20E-10	13.28	1.110E-06	28	5.6	1.548E-09	3.70E-10	23.90
29	5.8	2.369E-09	4.26E-10	17.99	1.110E-06	29	5.8	1.619E-09	3.77E-10	7.942E-07
30	6.0	2.025E-09	4.39E-10	21.64	1.111E-06	30	6.0	1.816E-09	3.82E-10	21.00
31	6.2	2.090E-09	4.29E-10	20.52	1.111E-06	31	6.2	1.857E-09	3.60E-10	19.35
32	6.4	2.144E-09	4.09E-10	19.07	1.111E-06	32	6.4	1.402E-09	3.31E-10	21.58
33	6.6	2.031E-09	3.89E-10	19.18	1.111E-06	33	6.6	8.188E-10	3.17E-10	38.63
34	6.8	1.722E-09	3.75E-10	21.52	1.112E-06	34	6.8	6.409E-10	3.16E-10	7.958E-07
35	7.0	1.180E-09	3.69E-10	31.33	1.112E-06	35	7.0	6.973E-10	3.15E-10	45.15
36	7.2	9.728E-10	3.73E-10	38.32	1.112E-06	36	7.2	6.931E-10	3.12E-10	45.06
37	7.4	1.363E-09	3.70E-10	27.15	1.113E-06	37	7.4	6.309E-10	3.06E-10	48.53
38	7.6	1.639E-09	3.48E-10	21.22	1.113E-06	38	7.6	5.928E-10	2.95E-10	49.67
39	7.8	1.375								

Table B-8

COMET: NEUTRON SPECTRUM AT 0 DEG & 200 CM

COMET NEUTRON SPECTRUM AT 45 DEG & 200 CM

GROUP	UPPER ENERGY (MEV)	PARTICLE FLUX (PARTICLES/CM ² -MEV-FISS)	ERROR (STD. DEV.)	RUNNING INTEGRAL (/CM ² -FISS)	UPPER ENERGY (MEV)	PARTICLE FLUX (PARTICLES/CM ² -MEV-FISS)	ERROR (STD. DEV.)	RUNNING INTEGRAL (/CM ² -FISS)
4	0.8	8.991E-08	1.64E-10	1.739E-08	4	0.8	1.886E-07	3.47E-10
5	1.0	4.589E-08	8.63E-11	2.717E-08	5	1.0	1.006E-07	1.65E-10
6	1.2	2.304E-08	7.08E-11	3.177E-08	6	1.2	5.642E-08	1.32E-10
7	1.4	1.366E-08	6.18E-11	0.31	7	1.4	3.076E-08	0.31
8	1.6	9.044E-09	5.63E-11	0.46	8	1.6	1.796E-08	1.04E-10
9	1.8	5.351E-09	4.59E-11	0.62	9	1.8	1.135E-08	9.12E-11
10	2.0	3.304E-09	4.48E-11	0.91	10	2.0	7.31E-09	6.27E-11
11	2.2	2.435E-09	4.29E-11	1.75	11	2.2	5.441E-09	7.66E-11
12	2.4	1.799E-09	4.09E-11	2.28	12	2.4	3.860E-09	7.18E-11
13	2.6	1.255E-09	3.90E-11	3.02	13	2.6	2.691E-09	6.66E-11
14	2.8	1.055E-09	3.69E-11	3.92	14	2.8	1.968E-09	6.68E-11
15	3.0	9.22E-10	4.33E-11	4.67	15	3.0	1.617E-09	6.97E-11
16	3.2	7.966E-10	4.62E-11	5.79	16	3.2	1.397E-09	7.32E-11
17	3.4	6.551E-10	4.33E-11	6.65	17	3.4	1.072E-09	7.32E-11
18	3.6	4.916E-10	4.05E-11	8.24	18	3.6	7.374E-10	6.25E-11
19	3.8	3.565E-10	4.05E-11	1.28	19	3.8	6.625E-10	6.06E-11
20	4.0	3.333E-10	4.08E-11	12.10	20	4.0	6.072E-10	5.913E-10
21	4.2	3.898E-10	4.11E-11	11.60	21	4.2	4.661E-10	5.19E-11
22	4.4	3.404E-10	4.09E-11	12.00	22	4.4	4.080E-10	5.19E-11
23	4.6	2.739E-10	4.03E-11	14.43	23	4.6	3.749E-10	5.30E-11
24	4.8	2.967E-10	3.95E-11	13.30	24	4.8	3.146E-10	5.04E-11
25	5.0	3.522E-10	3.82E-11	10.67	25	5.0	3.096E-10	4.65E-11
26	5.2	3.575E-10	3.64E-11	10.17	26	5.2	3.471E-10	4.65E-11
27	5.4	2.739E-10	3.59E-11	12.73	27	5.4	3.106E-10	4.88E-11
28	5.6	2.362E-10	3.45E-11	14.60	28	5.6	3.106E-10	4.88E-11
29	5.8	2.368E-10	3.56E-11	15.04	29	5.8	2.109E-10	4.57E-11
30	6.0	2.055E-10	3.68E-11	17.84	30	6.0	1.202E-10	4.062E-11
31	6.2	1.622E-10	3.65E-11	22.51	31	6.2	1.227E-10	4.68E-11
32	6.4	1.199E-10	3.59E-11	30.15	32	6.4	1.465E-10	4.54E-11
33	6.6	1.184E-10	3.59E-11	30.32	33	6.6	1.784E-10	4.39E-11
34	6.8	1.450E-10	3.62E-11	25.90	34	6.8	1.696E-10	4.31E-11
35	7.0	1.366E-10	3.67E-11	26.84	35	7.0	2.109E-10	4.57E-11
36	7.2	1.218E-10	3.74E-11	30.68	36	7.2	1.435E-10	4.39E-11
37	7.4	1.190E-10	3.77E-11	31.69	37	7.4	1.306E-10	4.22E-11
38	7.6	1.041E-10	3.73E-11	35.84	38	7.6	8.330E-11	4.14E-11
39	7.8	9.711E-11	3.67E-11	37.77	39	7.8	3.697E-11	4.08E-11
40	8.0	1.138E-10	3.58E-11	31.45	40	8.0	3.040E-11	3.99E-11
41	8.2	1.202E-10	3.46E-11	28.81	41	8.2	5.678E-11	3.82E-11
42	8.4	1.004E-10	3.37E-11	33.54	42	8.4	6.554E-11	3.68E-11
43	8.6	9.066E-11	3.32E-11	31.06	43	8.6	5.093E-11	3.61E-11
44	8.8	9.658E-11	3.25E-11	33.72	44	8.8	3.182E-11	3.55E-11
45	9.0	9.412E-11	3.18E-11	33.75	45	9.0	3.225E-11	3.422E-11
46	9.2	8.895E-11	3.10E-11	34.80	46	9.2	3.477E-11	3.38E-11
47	9.4	9.412E-11	3.04E-11	32.36	47	9.4	3.061E-11	3.22E-11
48	9.6	9.400E-11	3.00E-11	31.98	48	9.6	2.750E-11	3.21E-11
49	9.8	7.741E-11	2.92E-11	37.75	49	9.8	3.187E-11	3.18E-11
50	10.0	5.614E-11	2.89E-11	51.35	50	10.0	3.273E-11	3.12E-11

Table B-9

GROUP	UPPER ENERGY (MEV)	PARTICLE FLUX (PARTICLES/CM ² -MEV-FISS)	ERROR (STD. DEV.)	RUNNING INTEGRAL (/CM ² -FISS)	UPPER ENERGY (MEV)	PARTICLE FLUX (PARTICLES/CM ² -MEV-FISS)	ERROR (STD. DEV.)	RUNNING INTEGRAL (/CM ² -FISS)
4	0.8	1.739E-08	1.01E-10	1.739E-08	4	0.8	1.886E-07	3.47E-10
5	1.0	8.991E-08	6.63E-11	2.717E-08	5	1.0	1.006E-07	1.65E-10
6	1.2	4.589E-08	7.08E-11	3.177E-08	6	1.2	5.642E-08	1.32E-10
7	1.4	2.304E-08	6.18E-11	0.31	7	1.4	3.076E-08	0.31
8	1.6	9.044E-09	5.63E-11	0.46	8	1.6	1.796E-08	1.04E-10
9	1.8	5.351E-09	4.59E-11	0.62	9	1.8	1.135E-08	9.12E-11
10	2.0	3.304E-09	4.48E-11	0.91	10	2.0	7.31E-09	6.27E-11
11	2.2	2.435E-09	4.29E-11	1.75	11	2.2	5.441E-09	7.66E-11
12	2.4	1.799E-09	4.09E-11	2.28	12	2.4	3.860E-09	7.18E-11
13	2.6	1.255E-09	3.90E-11	3.02	13	2.6	2.691E-09	6.66E-11
14	2.8	1.055E-09	3.69E-11	3.92	14	2.8	1.968E-09	6.68E-11
15	3.0	9.22E-10	4.33E-11	4.67	15	3.0	1.617E-09	6.97E-11
16	3.2	7.966E-10	4.62E-11	5.79	16	3.2	1.397E-09	7.32E-11
17	3.4	6.551E-10	4.33E-11	6.65	17	3.4	1.072E-09	7.32E-11
18	3.6	4.916E-10	4.05E-11	8.24	18	3.6	7.374E-10	6.25E-11
19	3.8	3.565E-10	4.05E-11	11.28	19	3.8	6.625E-10	6.06E-11
20	4.0	3.333E-10	4.08E-11	12.10	20	4.0	6.072E-10	5.913E-10
21	4.2	3.898E-10	4.11E-11	11.60	21	4.2	4.661E-10	5.19E-11
22	4.4	3.404E-10	4.09E-11	12.00	22	4.4	4.080E-10	5.19E-11
23	4.6	2.739E-10	4.03E-11	14.43	23	4.6	3.749E-10	5.30E-11
24	4.8	2.967E-10	3.95E-11	13.30	24	4.8	3.146E-10	5.04E-11
25	5.0	3.522E-10	3.82E-11	10.67	25	5.0	3.096E-10	4.65E-11
26	5.2	3.575E-10	3.64E-11	10.17	26	5.2	3.471E-10	4.65E-11
27	5.4	2.739E-10	3.59E-11	12.73	27	5.4	3.106E-10	4.88E-11
28	5.6	2.362E-10	3.45E-11	14.60	28	5.6	3.106E-10	4.88E-11
29	5.8	2.368E-10	3.56E-11	15.04	29	5.8	2.109E-10	4.57E-11
30	6.0	2.055E-10	3.68E-11	17.84	30	6.0	1.202E-10	4.062E-11
31	6.2	1.622E-10	3.65E-11	22.51	31	6.2	1.227E-10	4.68E-11
32	6.4	1.199E-10	3.59E-11	30.15	32	6.4	1.465E-10	4.54E-11
33	6.6	1.184E-10	3.59E-11	30.32	33	6.6	3.106E-10	4.88E-11
34	6.8	1.450E-10	3.62E-11	25.90	34	6.8	1.696E-10	4.31E-11
35	7.0	1.366E-10	3.67E-11	26.84	35	7.0	2.109E-10	4.57E-11
36	7.2	1.218E-10	3.74E-11	30.68	36	7.2	1.435E-10	4.39E-11
37	7.4	1.190E-10	3.77E-11	31.69	37	7.4	1.306E-10	4.22E-11
38	7.6	1.041E-10	3.73E-11	35.84	38	7.6	8.330E-11	4.14E-11
39	7.8	9.711E-11	3.67E-11	37.77	39	7.8	3.697E-11	4.08E-11
40	8.0	1.138E-10	3.58E-11	31.45	40	8.0	3.040E-11	3.99E-11
41	8.2	1.202E-10	3.46E-11	28.81	41	8.2	5.678E-11	3.82E-11
42	8.4	1.004E-10	3.37E-11	33.54	42	8.4	6.554E-11	3.68E-11
43	8.6	9.066E-11	3.32E-11	36.76	43	8.6	5.093E-11	3.61E-11
44	8.8	9.658E-11	3.25E-11	33.72	44	8.8	3.182E-11	3.55E-11
45	9.0	9.412E-11	3.18E-11	33.75	45	9.0	3.225E-11	3.422E-11
46	9.2	8.895E-11	3.10E-11	34.80	46	9.2	3.477E-11	3.38E-11
47	9.4	9.412E-11	3.04E-11	32.36	47	9.4	3.061E-11	3.22E-11
48	9.6	9.400E-11	3.00E-11	31.98	48	9.6	2.750E-11	3.21E-11
49	9.8	7.741E-11	2.92E-11	37.75	49	9.8	3.187E-11	3.18E-11
50	10.0	5.614E-11	2.89E-11	51.35	50	10.0	3.273E-11	3.12E-11

3.76E-08

8.75E-08

8.73E-08

32.32

8.75E-08

31.05

8.76E-08

106.19

8.76E-08

29.87

8.73E-08

10.95

8.76E-08

110.05

8.76E-08

11.31

8.76E-08

29.56

8.76E-08

11.26

8.76E-08

8.76E-08

8.76E-08

8.76E-08

Table B-10

GROUP	UPPER ENERGY (MEV)	PARTICLE FLUX (PARTICLES/CM ² -MEV-FISS.)	ERROR (STD. DEV.)	RUNNING INTEGRAL (CM ² -FISS.)	COMET NEUTRON SPECTRUM AT 67.5 DEG & 200 CM
4	0.8	3.146E-07	6.31E-10	0.20	6.292E-08
5	1.0	3.724E-07	8.89E-10	0.23	9.739E-08
6	1.2	9.991E-08	3.19E-10	0.32	1.174E-07
7	1.4	5.520E-08	2.72E-10	0.49	1.284E-07
8	1.6	3.211E-08	2.51E-10	0.78	1.348E-07
9	1.8	2.102E-08	2.25E-10	1.07	1.390E-07
10	2.0	1.501E-08	2.04E-10	1.35	1.420E-07
11	2.2	1.068E-08	1.88E-10	1.75	1.442E-07
12	2.4	7.714E-09	1.75E-10	2.27	1.457E-07
13	2.6	5.689E-09	1.61E-10	2.84	1.468E-07
14	2.8	4.400E-09	1.60E-10	3.63	1.477E-07
15	3.0	3.310E-09	1.64E-10	4.95	1.484E-07
16	3.2	2.627E-09	1.71E-10	6.50	1.489E-07
17	3.4	2.225E-09	1.56E-10	7.02	1.494E-07
18	3.6	1.661E-09	1.42E-10	8.54	1.497E-07
19	3.8	1.274E-09	1.37E-10	10.74	1.500E-07
20	4.0	1.124E-09	1.34E-10	11.91	1.502E-07
21	4.2	1.104E-09	1.31E-10	11.86	1.504E-07
22	4.4	1.059E-09	1.27E-10	11.98	1.506E-07
23	4.6	8.754E-10	1.20E-10	13.15	1.508E-07
24	4.8	7.185E-10	1.14E-10	15.93	1.510E-07
25	5.0	6.607E-10	1.09E-10	16.47	1.511E-07
26	5.2	5.863E-10	1.04E-10	17.66	1.512E-07
27	5.4	5.033E-10	9.91E-11	19.68	1.513E-07
28	5.6	4.671E-10	9.56E-11	20.39	1.514E-07
29	5.8	4.280E-10	9.56E-11	22.42	1.515E-07
30	6.0	3.568E-10	9.91E-11	27.72	1.516E-07
31	6.2	3.175E-10	9.74E-11	30.56	1.516E-07
32	6.4	2.861E-10	9.30E-11	32.64	1.517E-07
33	6.6	2.654E-10	9.12E-11	34.39	1.518E-07
34	6.8	2.452E-10	9.56E-11	33.78	1.518E-07
35	7.0	2.618E-10	8.74E-11	33.37	1.518E-07
36	7.2	2.415E-10	8.64E-11	35.77	1.518E-07
37	7.4	1.945E-10	8.54E-11	43.93	1.519E-07
38	7.6	1.306E-10	8.14E-11	62.16	1.519E-07
39	7.8	9.465E-11	7.68E-11	81.13	1.519E-07
40	8.0	1.122E-10	7.31E-11	65.14	1.519E-07
41	8.2	1.295E-10	6.82E-11	53.64	1.520E-07
42	8.4	1.079E-10	6.26E-11	58.05	1.520E-07
43	8.6	1.011E-10	5.93E-11	58.67	1.520E-07
44	8.8	1.238E-10	5.60E-11	45.22	1.521E-07
45	9.0	1.248E-10	5.28E-11	42.35	1.521E-07
46	9.2	9.614E-11	5.18E-11	53.81	1.521E-07
47	9.4	6.768E-11	5.22E-11	77.16	1.521E-07
48	9.6	4.671E-11	5.01E-11	107.30	1.521E-07
49	9.8	3.073E-11	4.54E-11	147.52	1.521E-07
50	10.0	1.903E-11	4.23E-11	222.12	1.521E-07

Table B-11

GROUP	UPPER ENERGY (MEV)	PARTICLE FLUX (PARTICLES/CM ² -MEV-FISS.)	ERROR (STD. DEV.)	RUNNING INTEGRAL (CM ² -FISS.)	COMET NEUTRON SPECTRUM AT 90 DEG & 200 CM
4	0.8	3.146E-07	6.31E-10	0.20	6.292E-08
5	1.0	3.89E-10	0.23	9.739E-08	5.664E-07
6	1.2	9.991E-08	0.32	1.174E-07	3.56E-10
7	1.4	5.520E-08	0.49	1.284E-07	3.05E-10
8	1.6	3.211E-08	0.78	1.348E-07	4.010E-10
9	1.8	2.102E-08	1.07	1.390E-07	2.670E-10
10	2.0	1.501E-08	1.35	1.420E-07	2.54E-10
11	2.2	1.068E-08	1.75	1.442E-07	2.30E-10
12	2.4	7.714E-09	2.27	1.457E-07	2.14E-10
13	2.6	5.689E-09	2.84	1.468E-07	2.00E-10
14	2.8	4.400E-09	3.63	1.477E-07	1.85E-10
15	3.0	3.310E-09	4.95	1.484E-07	1.95E-10
16	3.2	2.627E-09	6.50	1.489E-07	2.00E-10
17	3.4	2.225E-09	7.02	1.494E-07	3.717E-09
18	3.6	1.661E-09	8.54	1.497E-07	2.832E-09
19	3.8	1.274E-09	10.74	1.500E-07	3.6
20	4.0	1.124E-09	11.91	1.502E-07	3.8
21	4.2	1.104E-09	11.86	1.504E-07	4.0
22	4.4	1.059E-09	11.98	1.506E-07	4.2
23	4.6	8.754E-10	12.0E-10	13.15	4.4
24	4.8	7.185E-10	11.4E-10	15.93	4.6
25	5.0	6.607E-10	10.9E-10	16.47	4.8
26	5.2	5.863E-10	10.4E-10	17.66	5.0
27	5.4	5.033E-10	9.91E-11	19.68	5.2
28	5.6	4.671E-10	9.56E-11	20.39	5.4
29	5.8	4.280E-10	9.56E-11	22.42	5.6
30	6.0	3.568E-10	9.91E-11	27.72	5.8
31	6.2	3.175E-10	9.74E-11	30.56	6.0
32	6.4	2.861E-10	9.30E-11	32.64	6.2
33	6.6	2.654E-10	9.12E-11	34.39	6.4
34	6.8	2.452E-10	9.56E-11	33.78	6.6
35	7.0	2.618E-10	8.74E-11	33.37	6.8
36	7.2	2.415E-10	8.64E-11	35.77	7.0
37	7.4	1.945E-10	8.54E-11	43.93	7.2
38	7.6	1.306E-10	8.14E-11	62.16	7.4
39	7.8	9.465E-11	7.68E-11	81.13	7.6
40	8.0	1.122E-10	7.31E-11	65.14	7.8
41	8.2	1.295E-10	6.82E-11	53.64	8.0
42	8.4	1.079E-10	6.26E-11	58.05	8.2
43	8.6	1.011E-10	5.93E-11	58.67	8.4
44	8.8	1.238E-10	5.60E-11	45.22	8.6
45	9.0	1.248E-10	5.28E-11	42.35	8.8
46	9.2	9.614E-11	5.18E-11	53.81	9.0
47	9.4	6.768E-11	5.22E-11	77.16	9.2
48	9.6	4.671E-11	5.01E-11	107.30	9.4
49	9.8	3.073E-11	4.54E-11	147.52	9.6
50	10.0	1.903E-11	4.23E-11	222.12	9.8

/CM2-FISS.)

(STD. DEV.)

DEV.)

/CM2-FISS.)

DEV.)

Table B-12

GROUP	UPPER ENERGY (MEV)	PARTICLE FLUX (PARTICLES/CM ² -MEV-FISS)	ERROR (STD. DEV.)	RUNNING INTEGRAL (/CM ² -FISS)	COMET NEUTRON SPECTRUM AT 112.5 DEG & 200 CM	GROUP	UPPER ENERGY (MEV)	PARTICLE FLUX (PARTICLES/CM ² -MEV-FISS)	ERROR (STD. DEV.)	RUNNING INTEGRAL (/CM ² -FISS)	
4	0.8	3.558E-07	7.00E-10	0.20	7.116E-08	4	0.8	2.881E-07	5.71E-10	0.20	5.761E-08
5	1.0	1.925E-07	4.16E-10	0.22	1.096E-07	5	1.0	1.512E-07	3.71E-10	0.25	8.789E-08
6	1.2	1.111E-07	3.40E-10	0.31	1.318E-07	6	1.2	8.368E-08	3.01E-10	0.36	1.046E-07
7	1.4	6.211E-08	2.90E-10	0.47	1.443E-07	7	1.4	4.569E-08	2.55E-10	0.56	1.138E-07
8	1.6	3.660E-08	2.68E-10	0.73	1.517E-07	8	1.6	2.633E-08	2.34E-10	0.89	1.190E-07
9	1.8	2.332E-08	2.39E-10	1.03	1.563E-07	9	1.8	1.679E-08	2.08E-10	1.24	1.224E-07
10	2.0	1.653E-08	2.18E-10	1.32	1.596E-07	10	2.0	1.178E-08	1.88E-10	1.59	1.247E-07
11	2.2	1.211E-08	2.02E-10	1.66	1.620E-07	11	2.2	8.229E-09	1.74E-10	2.11	1.264E-07
12	2.4	8.851E-09	1.89E-10	2.13	1.638E-07	12	2.4	5.871E-09	1.62E-10	2.77	1.275E-07
13	2.6	6.596E-09	1.74E-10	2.63	1.651E-07	13	2.6	4.235E-09	1.50E-10	3.55	1.284E-07
14	2.8	4.754E-09	1.72E-10	3.61	1.661E-07	14	2.8	3.261E-09	1.49E-10	4.57	1.290E-07
15	3.0	3.550E-09	1.77E-10	4.99	1.668E-07	15	3.0	2.532E-09	1.54E-10	6.06	1.296E-07
16	3.2	3.052E-09	1.85E-10	6.07	1.674E-07	16	3.2	2.084E-09	1.60E-10	7.67	1.300E-07
17	3.4	2.586E-09	1.69E-10	6.56	1.679E-07	17	3.4	1.702E-09	1.46E-10	8.54	1.303E-07
18	3.6	1.905E-09	1.54E-10	8.09	1.682E-07	18	3.6	1.327E-09	1.32E-10	9.97	1.305E-07
19	3.8	1.589E-09	1.48E-10	9.33	1.686E-07	19	3.8	9.633E-10	1.27E-10	13.24	1.308E-07
20	4.0	1.446E-09	1.45E-10	9.99	1.689E-07	20	4.0	7.811E-10	1.25E-10	16.08	1.309E-07
21	4.2	1.197E-09	1.41E-10	11.78	1.691E-07	21	4.2	7.806E-10	1.25E-10	15.90	1.311E-07
22	4.4	1.065E-09	1.38E-10	12.91	1.693E-07	22	4.4	7.816E-10	1.21E-10	15.49	1.312E-07
23	4.6	9.702E-10	1.32E-10	13.52	1.696E-07	23	4.6	7.820E-10	1.16E-10	17.17	1.314E-07
24	4.8	9.175E-10	1.25E-10	13.58	1.697E-07	24	4.8	5.477E-10	1.11E-10	20.15	1.315E-07
25	5.0	8.518E-10	1.18E-10	13.75	1.699E-07	25	5.0	5.875E-10	1.05E-10	19.20	1.316E-07
26	5.2	7.814E-10	1.11E-10	14.14	1.700E-07	26	5.2	5.518E-10	9.82E-11	17.86	1.317E-07
27	5.4	7.828E-10	1.04E-10	13.20	1.702E-07	27	5.4	4.784E-10	9.21E-11	19.34	1.318E-07
28	5.6	6.145E-10	9.65E-11	15.70	1.704E-07	28	5.6	3.875E-10	8.95E-11	23.16	1.318E-07
29	5.8	3.366E-10	9.65E-11	28.80	1.704E-07	29	5.8	3.127E-10	9.12E-11	29.08	1.319E-07
30	6.0	2.098E-10	1.01E-10	48.07	1.704E-07	30	6.0	2.237E-10	9.30E-11	41.66	1.319E-07
31	6.2	2.410E-10	1.01E-10	41.93	1.704E-07	31	6.2	1.583E-10	9.21E-11	52.41	1.320E-07
32	6.4	3.398E-10	9.82E-11	28.97	1.705E-07	32	6.4	1.504E-10	9.04E-11	59.89	1.320E-07
33	6.6	3.523E-10	9.39E-11	26.60	1.706E-07	33	6.6	1.461E-10	8.77E-11	60.27	1.321E-07
34	6.8	2.299E-10	9.12E-11	39.81	1.707E-07	34	6.8	1.673E-10	8.86E-11	52.73	1.321E-07
35	7.0	1.714E-10	9.30E-11	54.14	1.707E-07	35	7.0	2.118E-10	8.86E-11	41.72	1.321E-07
36	7.2	2.639E-10	9.39E-11	35.60	1.707E-07	36	7.2	1.911E-10	8.77E-11	46.02	1.322E-07
37	7.4	3.381E-10	9.21E-11	27.19	1.708E-07	37	7.4	1.411E-10	8.74E-11	61.94	1.322E-07
38	7.6	2.905E-10	8.55E-11	29.44	1.709E-07	38	7.6	1.196E-10	8.61E-11	71.98	1.322E-07
39	7.8	2.208E-10	7.89E-11	35.77	1.709E-07	39	7.8	9.28E-11	8.47E-11	91.36	1.322E-07
40	8.0	1.825E-10	7.37E-11	40.39	1.710E-07	40	8.0	6.153E-11	8.18E-11	132.98	1.322E-07
41	8.2	1.345E-10	6.91E-11	51.40	1.710E-07	41	8.2	4.489E-11	7.77E-11	173.11	1.323E-07
42	8.4	9.781E-11	6.66E-11	68.12	1.710E-07	42	8.4	3.897E-11	7.35E-11	188.54	1.323E-07
43	8.6	1.063E-10	6.47E-11	60.86	1.711E-07	43	8.6	5.15E-11	6.99E-11	136.60	1.323E-07
44	8.8	1.292E-10	6.11E-11	47.34	1.711E-07	44	8.8	8.904E-11	6.89E-11	77.45	1.323E-07
45	9.0	1.302E-10	5.62E-11	43.21	1.711E-07	45	9.0	1.117E-10	6.47E-11	61.19	1.324E-07
46	9.2	1.100E-10	5.22E-11	47.43	1.711E-07	46	9.2	8.308E-11	6.54E-11	78.81	1.324E-07
47	9.4	8.877E-11	5.06E-11	57.07	1.711E-07	47	9.4	4.221E-11	6.26E-11	148.32	1.324E-07
48	9.6	6.785E-11	5.05E-11	74.50	1.711E-07	48	9.6	3.339E-11	6.15E-11	184.10	1.324E-07
49	9.8	4.445E-11	5.03E-11	113.00	1.711E-07	49	9.8	5.438E-11	6.12E-11	112.59	1.324E-07
50	10.0	2.743E-11	4.79E-11	174.46	1.711E-07	50	10.0	7.090E-11	6.07E-11	85.63	1.324E-07

Table B-14

ANGLE-INTEGRATED NEUTRON SPECTRUM AT 75 CM					
GROUP	UPPER ENERGY (MEV)	LEAKAGE (NEUTRONS/MEV-FISS)	ERROR (STD. DEV.)	RUNNING INTEGRAL (N/FISS)	ERROR (%)
4	0.6	1.295E-01	1.15E-04	0.09	2.590E-02
5	1.0	7.264E-02	5.60E-05	0.08	4.043E-02
6	1.2	4.251E-02	4.33E-05	0.10	4.895E-02
7	1.4	2.379E-02	3.67E-05	0.15	5.370E-02
8	1.6	1.385E-02	3.38E-05	0.24	5.647E-02
9	1.8	9.026E-03	3.00E-05	0.33	5.822E-02
10	2.0	6.392E-03	2.69E-05	0.42	5.955E-02
11	2.2	4.633E-03	2.46E-05	0.53	6.048E-02
12	2.4	3.298E-03	2.28E-05	0.69	6.114E-02
13	2.6	2.298E-03	2.10E-05	0.91	6.160E-02
14	2.8	1.699E-03	2.10E-05	1.24	6.194E-02
15	3.0	1.379E-03	2.18E-05	1.58	6.221E-02
16	3.2	1.151E-03	2.27E-05	1.97	6.245E-02
17	3.4	9.228E-04	2.08E-05	2.25	6.263E-02
18	3.6	7.240E-04	1.89E-05	2.60	6.277E-02
19	3.8	5.968E-04	1.80E-05	3.02	6.289E-02
20	4.0	5.181E-04	1.75E-05	3.37	6.300E-02
21	4.2	4.431E-04	1.70E-05	3.84	6.309E-02
22	4.4	3.828E-04	1.66E-05	4.33	6.316E-02
23	4.6	3.561E-04	1.59E-05	4.44	6.324E-02
24	4.8	3.405E-04	1.49E-05	4.39	6.330E-02
25	5.0	3.063E-04	1.40E-05	4.58	6.336E-02
26	5.2	2.616E-04	1.32E-05	5.04	6.341E-02
27	5.4	2.332E-04	1.25E-05	5.57	6.346E-02
28	5.6	1.988E-04	1.19E-05	6.32	6.350E-02
29	5.8	1.599E-04	1.20E-05	7.54	6.353E-02
30	6.0	1.399E-04	1.23E-05	8.75	6.356E-02
31	6.2	1.281E-04	1.18E-05	9.24	6.369E-02
32	6.4	1.142E-04	1.12E-05	9.81	6.361E-02
33	6.6	9.877E-05	1.08E-05	10.88	6.352E-02
34	6.8	8.156E-05	1.05E-05	11.76	6.364E-02
35	7.0	6.297E-05	1.04E-05	12.51	6.366E-02
36	7.2	7.682E-05	1.03E-05	13.33	6.368E-02
37	7.4	7.196E-05	1.00E-05	13.92	6.369E-02
38	7.6	6.731E-05	9.56E-06	14.22	6.370E-02
39	7.8	5.972E-05	9.04E-06	15.13	6.372E-02
40	8.0	4.907E-05	8.11E-06	17.35	6.374E-02
41	8.2	4.228E-05	8.11E-06	19.18	6.374E-02
42	8.4	3.955E-05	7.74E-06	19.57	6.375E-02
43	8.6	3.648E-05	7.39E-06	20.25	6.375E-02
44	8.8	3.445E-05	7.11E-06	20.66	6.375E-02
45	9.0	3.220E-05	6.82E-06	21.19	6.375E-02
46	9.2	2.662E-05	6.50E-06	24.40	6.376E-02
47	9.4	2.155E-05	6.22E-06	28.71	6.377E-02
48	9.6	2.096E-05	6.10E-06	29.06	6.377E-02
49	9.8	2.082E-05	5.90E-06	28.37	6.378E-02
50	10.0	1.914E-05	5.78E-06	30.20	6.378E-02

Table B-15

ANGLE-INTEGRATED NEUTRON SPECTRUM AT 200 CM					
GROUP	UPPER ENERGY (MEV)	LEAKAGE (NEUTRONS/MEV-FISS)	ERROR (STD. DEV.)	RUNNING INTEGRAL (N/FISS)	ERROR (%)
4	0.8	1.295E-01	1.15E-04	0.09	2.590E-02
5	1.0	7.264E-02	5.60E-05	0.08	4.043E-02
6	1.2	4.251E-02	4.33E-05	0.10	4.895E-02
7	1.4	2.379E-02	3.67E-05	0.15	5.370E-02
8	1.6	1.385E-02	3.38E-05	0.24	5.647E-02
9	1.8	9.026E-03	3.00E-05	0.33	5.822E-02
10	2.0	6.392E-03	2.69E-05	0.42	5.955E-02
11	2.2	4.633E-03	2.46E-05	0.53	6.048E-02
12	2.4	3.298E-03	2.10E-05	0.91	6.160E-02
13	2.6	2.298E-03	2.10E-05	1.24	6.194E-02
14	2.8	1.699E-03	2.18E-05	1.58	6.221E-02
15	3.0	1.379E-03	2.18E-05	1.97	6.245E-02
16	3.2	1.151E-03	2.27E-05	1.97	6.245E-02
17	3.4	9.228E-04	2.08E-05	2.25	6.263E-02
18	3.6	7.240E-04	1.89E-05	2.60	6.277E-02
19	3.8	5.968E-04	1.80E-05	3.02	6.289E-02
20	4.0	5.181E-04	1.75E-05	3.37	6.300E-02
21	4.2	4.431E-04	1.70E-05	3.84	6.309E-02
22	4.4	3.828E-04	1.66E-05	4.33	6.316E-02
23	4.6	3.561E-04	1.59E-05	4.44	6.324E-02
24	4.8	3.405E-04	1.49E-05	4.39	6.330E-02
25	5.0	3.063E-04	1.40E-05	4.58	6.336E-02
26	5.2	2.616E-04	1.32E-05	5.04	6.341E-02
27	5.4	2.332E-04	1.25E-05	5.57	6.346E-02
28	5.6	1.988E-04	1.19E-05	6.32	6.350E-02
29	5.8	1.599E-04	1.20E-05	7.54	6.353E-02
30	6.0	1.399E-04	1.23E-05	8.75	6.356E-02
31	6.2	1.281E-04	1.18E-05	9.24	6.369E-02
32	6.4	1.142E-04	1.12E-05	9.81	6.361E-02
33	6.6	9.877E-05	1.08E-05	10.88	6.352E-02
34	6.8	8.156E-05	1.05E-05	11.76	6.364E-02
35	7.0	6.297E-05	1.04E-05	12.51	6.366E-02
36	7.2	7.682E-05	1.03E-05	13.33	6.368E-02
37	7.4	7.196E-05	1.00E-05	13.92	6.369E-02
38	7.6	6.731E-05	9.56E-06	14.22	6.370E-02
39	7.8	5.972E-05	9.04E-06	15.13	6.372E-02
40	8.0	4.907E-05	8.11E-06	17.35	6.374E-02
41	8.2	4.228E-05	8.11E-06	19.18	6.374E-02
42	8.4	3.955E-05	7.74E-06	19.57	6.375E-02
43	8.6	3.648E-05	7.39E-06	20.25	6.375E-02
44	8.8	3.445E-05	7.11E-06	20.66	6.375E-02
45	9.0	3.220E-05	6.82E-06	21.19	6.375E-02
46	9.2	2.662E-05	6.50E-06	24.40	6.376E-02
47	9.4	2.155E-05	6.22E-06	28.71	6.377E-02
48	9.6	2.096E-05	6.10E-06	29.06	6.377E-02
49	9.8	2.082E-05	5.90E-06	28.37	6.378E-02
50	10.0	1.914E-05	5.78E-06	30.20	6.378E-02

ANGLE-INTEGRATED NEUTRON SPECTRUM AT 200 CM					
GROUP	UPPER ENERGY (MEV)	LEAKAGE (NEUTRONS/MEV-FISS)	ERROR (STD. DEV.)	RUNNING INTEGRAL (N/FISS)	ERROR (%)
4	0.8	1.295E-01	1.15E-04	0.09	2.590E-02
5	1.0	7.264E-02	5.60E-05	0.08	4.043E-02
6	1.2	4.251E-02	4.33E-05	0.10	4.895E-02
7	1.4	2.379E-02	3.67E-05	0.15	5.370E-02
8	1.6	1.385E-02	3.38E-05	0.24	5.647E-02
9	1.8	9.026E-03	3.00E-05	0.33	5.822E-02
10	2.0	6.392E-03	2.69E-05	0.42	5.955E-02
11	2.2	4.633E-03	2.46E-05	0.53	6.048E-02
12	2.4	3.298E-03	2.10E-05	0.91	6.160E-02
13	2.6	2.298E-03	2.10E-05	1.24	6.194E-02
14	2.8	1.699E-03	2.18E-05	1.58	6.221E-02
15	3.0	1.379E-03	2.18E-05	1.97	6.245E-02
16	3.2	1.151E-03	2.27E-05	1.97	6.245E-02
17	3.4	9.228E-04	2.08E-05	2.25	6.263E-02
18	3.6	7.240E-04	1.89E-05	2.60	6.277E-02
19	3.8	5.968E-04	1.80E-05	3.02	6.289E-02
20	4.0	5.181E-04	1.75E-05	3.37	6.300E-02
21	4.2	4.431E-04	1.70E-05	3.84	6.309E-02
22	4.4	3.828E-04	1.66E-05	4.33	6.316E-02
23	4.6	3.561E-04	1.59E-05	4.44	6.324E-02
24	4.8	3.405E-04	1.49E-05	4.39	6.330E-02
25	5.0	3.063E-04	1.40E-05	4.58	6.336E-02
26	5.2	2.616E-04	1.32E-05	5.04	6.341E-02
27	5.4	2.332E-04	1.25E-05	5.57	6.346E-02
28	5.6	1.988E-04	1.19E-05	6.32	6.350E-02
29	5.8	1.599E-04	1.20E-05	7.54	6.353E-02
30	6.0	1.399E-04	1.23E-05	8.75	6.356E-02
31	6.2	1.281E-04	1.18E-05	9.24	6.369E-02
32	6.4	1.142E-04	1.12E-05	9.81	6.361E-02
33	6.6	9.877E-05	1.08E-05	10.88	6.352E-02
34	6.8	8.156E-05	1.05E-05	11.76	6.364E-02
35	7.0	6.297E-05	1.04E-05	12.51	6.366E-02
36	7.2	7.682E-05	1.03E-05	13.33	6.368E-02
37	7.4	7.196E-05	1.00E-05	13.92	6.369E-02
38	7.6	6.731E-05	9.56E-06	14.22	6.370E-02
39	7.8	5.972E-05	9.04E-06	15.13	6.372E-02
40	8.0	4.907E-05	8.11E-06	17.35	6.374E-02
41	8.2	4.228E-05	8.11E-06	19.18	6.374E-02
42	8.4	3.955E-05	7.74E-06	19.57	6.375E-02
43	8.6	3.648E-05	7.39E-06	20.25	6.375E-02
44	8.8	3.445E-05	7.11E-06	20.66	6.375E-02
45	9.0	3.220E-05	6.82E-06	21.19	6.375E-02
46	9.2	2.662E-05	6.50E-06	24.40	6.376E-02
47	9.4	2.155E-05	6.22E-06	28.71	6.377E-02
48	9.6	2.096E-05	6.10E-06	29.06	6.377E-02
49	9.8	2.082E-05	5.90E-06	28.37	6.378E-02
50	10.0	1.914E-05	5.78E-06		

APPENDIX C : Boron-triflouride Detector Efficiency

Plotted and listed in this appendix is the energy-dependent efficiency of the cadmium-covered boron-triflouride detector used for integral determinations, as described in the main text. The detector is essentially insensitive to neutrons of energies below 0.5 electron-volts due to the exterior 1-mm cadmium encapsulation. Above this energy the response decreases approximately as the inverse of neutron velocity (or square root of energy). Absolute calibration of this detector has been made to within 5 % by comparison to the National Thermal Neutron Standard at the National Research Council of Canada. The effective number of boron-10 nuclei contributing to the detector response (above a repeatable pulse-height bias level of one-fourth of the alpha-particle peak) has been established as $9.10E+20$ nuclei. The efficiencies listed have been determined by multiplying this number by the (n,α) cross-section of boron-10 and then the transmission probability through the 1-mm thickness of cadmium, for each neutron energy. The quoted units of efficiency are therefore centimeters-squared, which when integrated against a calculated neutron fluence with units of neutrons/cm².MeV, will predict total counts recorded by the detector.

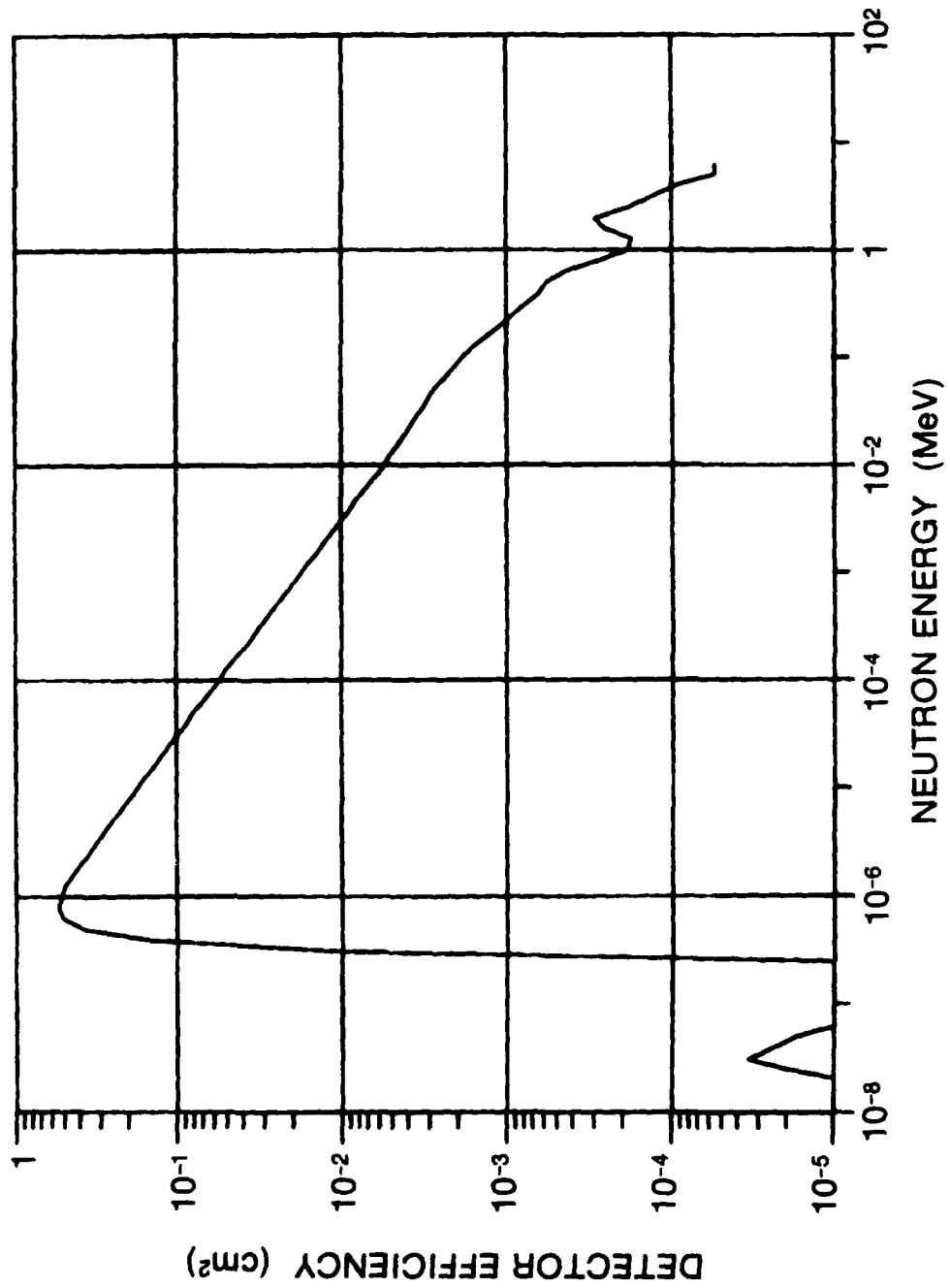


Figure C-1 : Energy-dependent detection efficiency for the Cd-covered BF_3 detector.

Table C-1 : Energy-dependent detection efficiency for the cadmium-covered boron-triflouride detector.

Energy (MeV)	Efficiency (cm ²)	Energy (MeV)	Efficiency (cm ²)
1.000E-09	6.308E-16	1.000E-04	5.535E-02
1.259E-09	1.089E-14	1.259E-04	4.933E-02
1.585E-09	1.490E-13	1.585E-04	4.397E-02
1.995E-09	1.647E-12	1.995E-04	3.919E-02
2.512E-09	1.495E-11	2.512E-04	3.493E-02
3.162E-09	1.311E-10	3.162E-04	3.113E-02
3.981E-09	7.243E-10	3.981E-04	2.774E-02
5.012E-09	3.974E-09	5.012E-04	2.473E-02
6.310E-09	1.891E-08	6.310E-04	2.204E-02
7.943E-09	7.892E-08	7.943E-04	1.964E-02
1.000E-08	2.919E-07	1.000E-03	1.750E-02
1.259E-08	9.659E-07	1.259E-03	1.560E-02
1.585E-08	2.884E-06	1.585E-03	1.390E-02
1.995E-08	7.834E-06	1.995E-03	1.239E-02
2.512E-08	1.950E-05	2.512E-03	1.104E-02
3.162E-08	3.446E-05	3.162E-03	9.843E-03
3.981E-08	2.435E-05	3.981E-03	8.773E-03
5.012E-08	1.713E-05	5.012E-03	7.819E-03
6.310E-08	9.639E-06	6.310E-03	6.969E-03
7.943E-08	2.293E-06	7.943E-03	6.211E-03
1.000E-07	7.098E-08	1.000E-02	5.535E-03
1.259E-07	3.955E-11	1.259E-02	5.006E-03
1.585E-07	9.004E-16	1.585E-02	4.525E-03
1.995E-07	2.750E-13	1.995E-02	4.090E-03
2.512E-07	1.109E-05	2.512E-02	3.697E-03
3.162E-07	1.045E-02	3.162E-02	3.342E-03
3.981E-07	1.457E-01	3.981E-02	3.021E-03
5.012E-07	3.847E-01	5.012E-02	2.729E-03
6.310E-07	5.095E-01	6.309E-02	2.388E-03
7.943E-07	5.350E-01	7.943E-02	2.090E-03
1.000E-06	5.156E-01	1.000E-01	1.829E-03
1.259E-06	4.868E-01	1.259E-01	1.557E-03
1.585E-06	4.386E-01	1.585E-01	1.301E-03
1.995E-06	3.917E-01	1.995E-01	1.086E-03
2.512E-06	3.493E-01	2.512E-01	9.072E-04
3.162E-06	3.113E-01	3.162E-01	7.577E-04
3.981E-06	2.774E-01	3.981E-01	6.328E-04
5.012E-06	2.473E-01	5.012E-01	5.557E-04
6.310E-06	2.204E-01	6.309E-01	4.418E-04
7.943E-06	1.964E-01	7.943E-01	2.837E-04
1.000E-05	1.750E-01	1.000E-00	1.822E-04
1.259E-05	1.560E-01	1.259E-00	1.759E-04
1.585E-05	1.320E-01	1.585E-00	2.530E-04
1.995E-05	1.239E-01	1.995E-00	2.889E-04
2.512E-05	1.104E-01	2.512E-00	1.783E-04
3.162E-05	9.843E-02	3.162E-00	1.333E-04
3.981E-05	8.773E-02	3.981E-00	9.333E-05
5.012E-05	7.819E-02	5.012E-00	5.466E-05
6.310E-05	6.969E-02	6.309E-00	5.466E-05
7.943E-05	6.211E-02	7.943E-00	5.466E-05
		1.000E-01	5.466E-05

UNCLASSIFIED

Security Classification

DOCUMENT CONTROL DATA - R & D		
(Security classification of title, body of abstract and indexing annotation must be entered when the overall document is classified)		
1 ORIGINATING ACTIVITY DEFENCE RESEARCH ESTABLISHMENT OTTAWA Ottawa, Ontario, K1A 0Z4, CANADA	2a DOCUMENT SECURITY CLASSIFICATION Unclassified	2b GROUP
3 DOCUMENT TITLE NEUTRON LEAKAGE FROM "COMET" - A DUPLICATE LITTLE-BOY DEVICE		
4 DESCRIPTIVE NOTES (Type of report and inclusive dates) REPORT		
5 AUTHOR(S) (Last name, first name, middle initial) Robitaille, H. Alan and Hoffarth, Bernard E.		
6 DOCUMENT DATE December 1983	7a TOTAL NO OF PAGES 37	7b NO OF REFS 16
8a PROJECT OR GRANT NO 11A	9a ORIGINATOR'S DOCUMENT NUMBER(S) DREO Report 878	
8b CONTRACT NO	9b OTHER DOCUMENT NO(S) (Any other numbers that may be assigned this document)	
10 DISTRIBUTION STATEMENT Unlimited		
11 SUPPLEMENTARY NOTES	12. SPONSORING ACTIVITY CRAD/DREO	
13 ABSTRACT Fast neutron spectra between 600 keV and 10 MeV, directed outwards from the surface of the "COMET" assembly, were measured using an NE-213 fast-neutron spectrometer at the Los Alamos National Laboratory. The COMET experiment, consisting of a duplicate Little-Boy device suitably modified for operation in the delayed-critical regime, was to provide improved energy and angular distributions of leakage spectra in support of efforts to re-evaluate ground doses from the Hiroshima bombing.		
Measurements were obtained at seven polar angles (from 0 to 135 degrees) and at two radii from the centre of the active volume (75 and 200 centimeters). These measurements were compared to two calculations available at the time of writing; one an earlier (1976) one-dimensional estimation and another more recent (1982) two-dimensional calculation, both based on Monte-Carlo techniques. Differences in high-energy neutron leakage are apparent and probably due to dynamical considerations, as the theoretical calculations simulated the disassembling weapon itself, rather than the static experiments described herein.		

UNCLASSIFIED

Security Classification

KEY WORDS

Neutron
 Nuclear Weapon
 Hiroshima
 Radiation
 COMET
 Neutron Spectrum

INSTRUCTIONS

1. ORIGINATING ACTIVITY Enter the name and address of the organization issuing the document.
- 2a. DOCUMENT SECURITY CLASSIFICATION Enter the overall security classification of the document including special warning terms whenever applicable.
- 2b. GROUP Enter security reclassification group number. The three groups are defined in Appendix 'M' of the DRB Security Regulations
3. DOCUMENT TITLE Enter the complete document title in all capital letters. Titles in all cases should be unclassified. If a sufficiently descriptive title cannot be selected without classification, show title classification with the usual one capital-letter abbreviation in parentheses immediately following the title.
4. DESCRIPTIVE NOTES Enter the category of document, e.g. technical report, technical note or technical letter. If appropriate, enter the type of document, e.g. interim, progress, summary, annual or final. Give the inclusive dates when a specific reporting period is covered.
5. AUTHOR(S): Enter the name(s) of author(s) as shown on or in the document. Enter last name, first name, middle initial. If military, show rank. The name of the principal author is an absolute minimum requirement.
6. DOCUMENT DATE Enter the date (month, year) of Establishment approval for publication of the document.
- 7a. TOTAL NUMBER OF PAGES The total page count should follow normal pagination procedures, i.e., enter the number of pages containing information.
- 7b. NUMBER OF REFERENCES Enter the total number of references cited in the document.
- 8a. PROJECT OR GRANT NUMBER: If appropriate, enter the applicable research and development project or grant number under which the document was written.
- 8b. CONTRACT NUMBER If appropriate, enter the applicable number under which the document was written.
- 9a. ORIGINATOR'S DOCUMENT NUMBER(S) Enter the official document number by which the document will be identified and controlled by the originating activity. This number must be unique to this document.
- 9b. OTHER DOCUMENT NUMBER(S) If the document has been assigned any other document numbers (either by the originator or by the sponsor), also enter this number(s).
10. DISTRIBUTION STATEMENT Enter any limitations on further dissemination of the document, other than those imposed by security classification, using standard statements such as
 - (1) "Qualified requesters may obtain copies of this document from their defence documentation center."
 - (2) "Announcement and dissemination of this document is not authorized without prior approval from originating activity."
11. SUPPLEMENTARY NOTES Use for additional explanatory notes.
12. SPONSORING ACTIVITY Enter the name of the departmental project office or laboratory sponsoring the research and development. Include address.
13. ABSTRACT Enter an abstract giving a brief and factual summary of the document, even though it may also appear elsewhere in the body of the document itself. It is highly desirable that the abstract of classified documents be unclassified. Each paragraph of the abstract shall end with an indication of the security classification of the information in the paragraph (unless the document itself is unclassified) represented as (TS), (S), (C), (R), or (U).

The length of the abstract should be limited to 20 single-spaced standard typewritten lines; 7½ inches long.

14. KEY WORDS: Key words are technically meaningful terms or short phrases that characterize a document and could be helpful in cataloging the document. Key words should be selected so that no security classification is required. Identifiers, such as equipment model designation, trade name, military project code name, geographic location, may be used as key words but will be followed by an indication of technical context.